Friction **12**(1): 1–38 (2024)
https://doi.org/10.1007/s40544-022-0707-5
ISSN 2223-7690
CN 10-1237/TH
REVIEW ARTICLE

Review of the evolution and prevention of friction, wear, and noise for water-lubricated bearings used in ships

Zhuo ZHANG[1], **Wu OUYANG**[1,2,4,*], **Xingxin LIANG**[2,3,4], **Xinping YAN**[1,2,4], **Chengqin YUAN**[1,2,4], **Xincong ZHOU**[1,2,4], **Zhiwei GUO**[1,2,4], **Conglin DONG**[1,2,4], **Zhenglin LIU**[1], **Yong JIN**[1], **Jinhua XIAO**[1]

[1] *School of Transportation and Logistics Engineering, Wuhan University of Technology, Wuhan 430063, China*
[2] *Reliability Engineering Institute, National Engineering Research Center for Water Transport Safety, Wuhan 430063, China*
[3] *School of Naval Architecture, Ocean and Energy Power Engineering, Wuhan University of Technology, Wuhan 430063, China*
[4] *East Lake Laboratory, Wuhan 420202, China*

Received: 14 July 2022 / Revised: 08 September 2022 / Accepted: 05 October 2022

Abstract: With the development of green tribology in the shipping industry, the application of water lubrication gradually replaces oil lubrication in stern bearings and thrust bearings. In terms of large-scale and high-speed ships, water-lubricated bearings with high performance are more strictly required. However, due to the lubricating medium, water-lubricated bearings have many problems such as friction, wear, vibration, noise, etc. This review focuses on the performance of marine water-lubricated bearings and their failure prevention mechanism. Furthermore, the research of marine water-lubricated bearings is reviewed by discussing its lubrication principle, test technology, friction and wear mechanism, and friction noise generation mechanism. The performance enhancement methods have been overviewed from structure optimization and material modification. Finally, the potential problems and the perspective of water-lubricated bearings are given in detail.

Keywords: water-lubricated bearings; lubrication principles; test techniques; friction and wear; friction noise; evolution and prevention

1 Introduction

The applications of water-lubricated bearings (WLBs) originated from the early days of ship propulsion. As shown in Fig. 1, WLBs have evolved with the developing materials and related technologies to form a rich spectrum of products, which mainly belong to radial sliding bearings and are used for ship propulsion system stern bearing. With the advancement and application of shaftless rim-driven thruster (RDT), the WLBs in ships began to extend their application fields from journal bearings to thrust bearings.

It is necessary to protect the environment and resources that oil-lubricated bearings need to be replaced because they might consume massive mineral oil and precious metal resources. It has been a trend to replace oil-lubricated bearings with WLBs in the marine field because they meet the requirements of green shipping [1]. The complex structure makes it difficult for oil-lubricated metal bearings to reduce friction, wear, vibration, shock, and noise. But the simple structure WLBs with polymer bearing materials such as rubber have significant advantages in these areas. However, as shown in Fig. 2, due to the low viscosity of lubrication water and its harsh operating environment and working conditions [2, 3], there are some problems with friction wear and vibration noise. Further research on the materials and structure of WLBs is required for the lower vibration and noise and less friction and wear to improve the operational performance and service life.

In general, WLBs need the performance of low

* Corresponding author: Wu OUYANG, E-mail: ouyangw@whut.edu.cn

Nomenclature

WLBs	Water-lubricated bearings	SEHL	Soft elastohydrodynamic lubrication
WLSBs	Water-lubricated stern bearings	ML	Mixed lubrication
HD	Hydrodynamic lubrication	L/D	Length-to-diameter ratio
EHL	Elastohydrodynamic lubrication	RDT	Shaftless rim-driven thruster
THD	Thermohydrodynamic lubrication	NBR	Nitrile butadiene rubber
TEHD	Thermoelastic hydrodynamic lubrication		

friction, high wear resistance, low vibration, and low noise to achieve high-efficiency operation. Under the great application demands, WLBs have attracted extensive attention from relevant universities and institutes to study its materials, structures, and test techniques. This paper would introduce the lubrication theories, characteristic simulations, test devices, and performance test method, and review the research progress and development trend of marine WLBs performance evolution and prevention mechanism, method and technology of the friction, wear, and vibration noise.

2 Lubrication theories and characteristic simulations of WLBs

2.1 Lubrication theories

Under the low speed and heavy load, the water-lubrication film of WLBs is thin, which is difficult to form an effective lubrication film. Moreover, the bearing bush generally adopts polymer composite materials, which is easy to be large deformation. Therefore, it is necessary to establish elastohydrodynamic lubrication (EHL) and mixed lubrication (ML) models.

2.1.1 *Hydrodynamic lubrication theories*

The differential equation derived by Reynolds for fluid film pressure distribution provided a solution for hydrodynamic lubrication (HD) theory. The engineering application of HD theory was promoted by the infinite length bearings theory [4] and the analytical formula for short bearings [5]. Subsequently, the models of EHL, thermohydrodynamic lubrication (THD), thermoelastic hydrodynamic lubrication (TEHD), and soft elastohydrodynamic lubrication (SEHL) were further developed with material

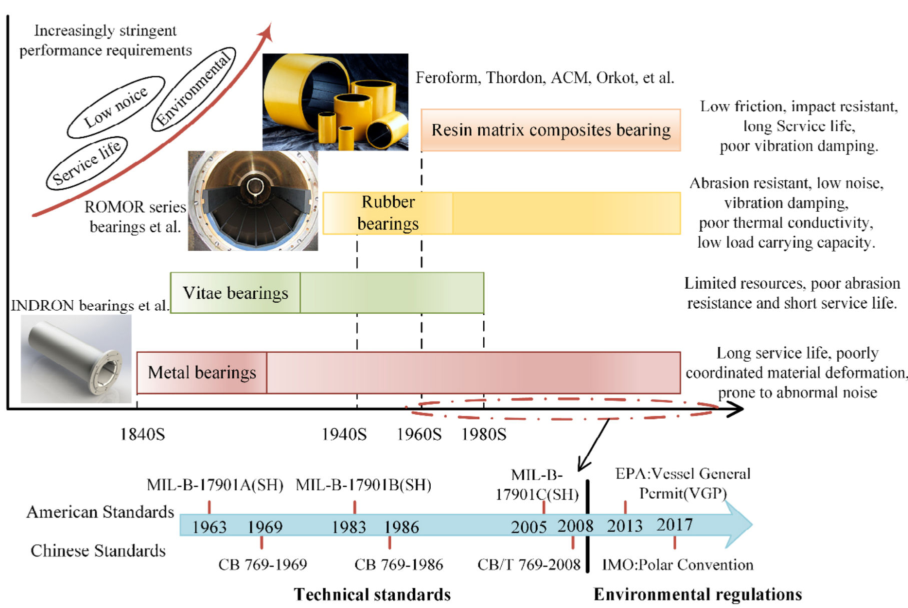

Fig. 1 Different development stages of WLBs.

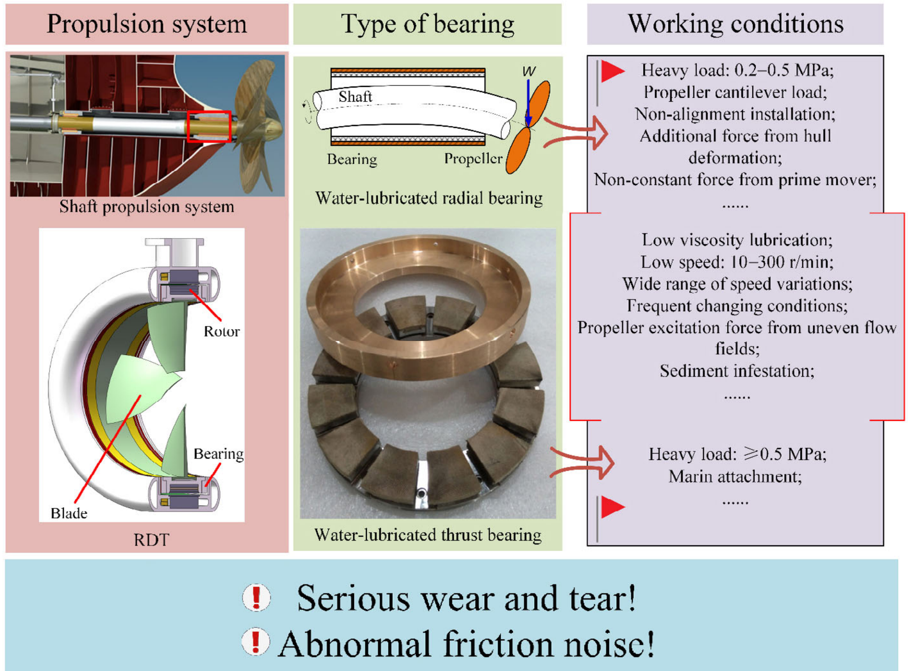

Fig. 2 Application of WLBs in ship propulsion systems and main problems.

properties, heat transfer, and other factors considered. The theoretical studies were shown in Table 1.

Table 1 shows that the hydrodynamic lubrication theories are gradually developed by considering practical influencing factors on the basis of a simplified and idealized theoretical model. But it cannot fully reflect the actual situation. When the peak contact appears at the rough micro-body of the lubrication surface, it would be difficult to analyze the performance of the bearings by the EHL model, which requires partial elastohydrodynamic lubrication (PEHL) or ML theory.

2.1.2 Mixed lubrication theories

ML introduces a rough surface contact model to consider hydrodynamic and surface contact pressures based on the EHL or TEHD model, so it is difficult for ML to describe the rough surface and simultaneously solve these two pressures. According to the description method of surface roughness, the ML model could be divided into statistical and deterministic models, and the related studies [11, 23–35] were shown in Fig. 3.

The Patir-Cheng (PC) flow model is a typical representative of the statistical model. From this model, the average contact pressure can be obtained by the average clearance from the average Reynolds equation. The contact factor of the PC flow model makes the mean Reynolds equation more suitable for partial hydrodynamic (PHD) and PEHL. Venner et al. [33] argued that the PC flow model failed to consider the elastic deformation of the microgeometry, and the orientation parameter cannot uniquely define the roughness direction so that different roughness profiles might have the same statistical properties. These two disadvantages caused that the "averaging treatment" of the PC flow method could not solve the ML model well. The improving surface topography observation capability has enabled techniques such as optical interferometry [36, 37], and thin film colorimetric interferometry [38] to be applied for surface roughness, which has attracted attention to deterministic models of roughness for micro-EHL studies [33, 34].

Conventional ML models are incompletely suitable for marine water lubricated stern bearings (WLSBs) because those only consider microscopic ML in line or point contact. As shown in Fig. 4, shaft tilt and large deformations could also lead to macroscopic surface contact in the partial area [2]. In this case, it is meaningful to distinguish the contact zone by lubrication state as mentioned in Refs. [39, 40]. Ouyang et al. [41] firstly proposed that a distributed parameter lubrication model should be established

Table 1 Theoretical study on hydrodynamic lubrication.

Type	Characteristics		Results		Ref.
Solution of Reynolds equation	Difference method	Swift-Stieber boundary conditions	Could deal with the cavitation-occurring part		[6]
	Mean velocity method		Complete kinematic analysis of short journal bearings		[7]
	Consider the additional mass of the lubricant and turbulence effects		Extended short bearing theory to finite length bearings		[8]
EHL model	The max elastic deformation of rubber lining is greater than the min water film thickness		The elastic flow-pressure lubrication calculation scheme		[9]
	Considering the local wear of the pad edge	EHL+LW model	Improve the loading capacity prediction accuracy		[10]
	Red-black successive over-relaxation method	High-density EHL mesh	Describe the textural features of the bearing surface effectively		[11]
SEHL model	Transformed into a calculation problem of dry contact pressure under certain conditions		Greatly simplifying the calculation process		[12]
	Multiple meshes numerical method		The effect of surface roughness		[13]
	Consider the local attenuation and complementary waves				[14]
THD model	Isothermal assumption	"Effective temperature" to "effective viscosity"	Calculated the loading capacity	Only consider the temperature-viscosity effect	[15]
	Consider the heat conduction		Reynolds equation considering the variation of viscosity with film thickness		[16]
	Finite difference method FDM	Walther temperature-viscosity equation	Analyzed the performance of thermodynamic pressure lubrication		[17]
TEHD	FDM and FEM		The accuracy improved	Defects in the calculation of thermal effects	[18]
	FDM-FEM coupled		The accuracy improved	Could not reflect the influence of bearing face geometry well	[19, 20]
	CFD-FEM coupled		Simultaneous solution and coupling of flow and solid models	High mesh quality requirements, long solution time, and difficulty in convergence	[21, 22]

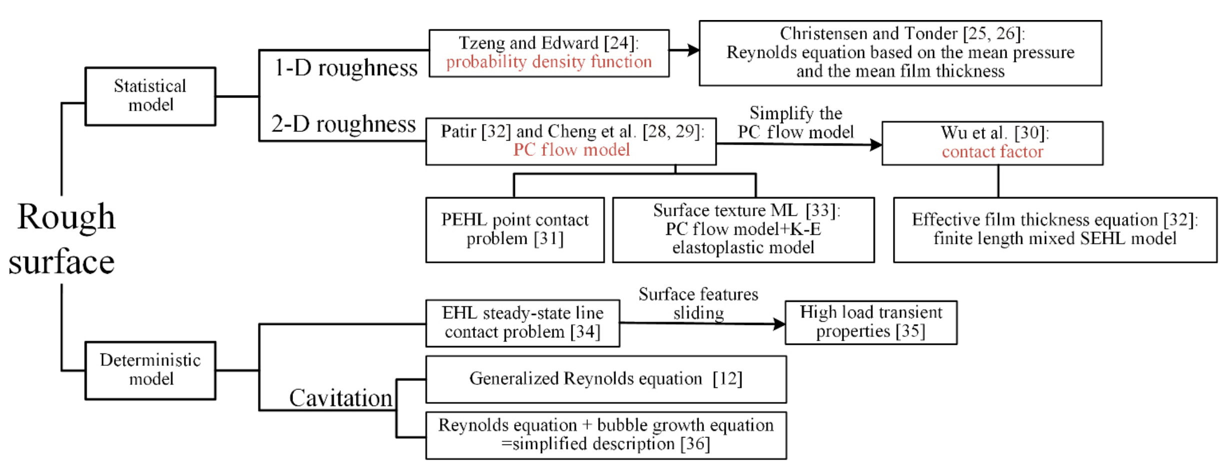

Fig. 3 Theoretical studies on mixed lubrication based on surface roughness.

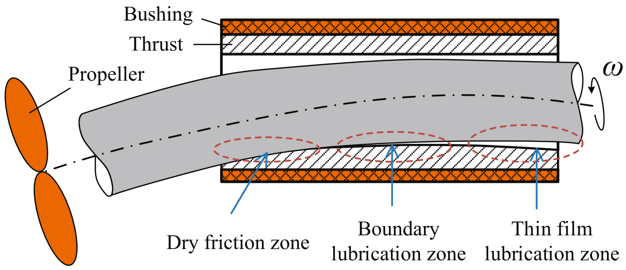

Fig. 4 Mixed lubrication state on the interface of WLSBs.

for partial fluid film lubrication. It is meaningful to introduce distribution characteristic parameters into the basic lubrication equation to analyze the different lubrication zones. Li et al. obtained the film thickness distribution of the full bearing by the circumferential film thickness of three interfaces, which identified the distributed lubrication characteristics of the WLBs [42].

2.1.3 *Solution algorithms*

The lubrication theories of WLBs and their control equations could be summarized as shown in Fig. 5. A variety of solution algorithms for lubrication models have been developed just as shown in Table 2.

As one of the representatives of the ML model, more rigorous mathematical derivation was needed by the PC flow model to calculate the flow factor with the effects of micro-cavitation and elastic-plastic deformation of rough surfaces [53]. The deterministic models have been developed with the surface profile recognition technologies, its further development depends on more accurate surface identification, better surface roughness mathematical models, and solution methods. The researches on distributed lubrication only present the modeling concept and simple calculation, which needs to be further proposed by the complete equations and algorithms. It is necessary to develop the solving algorithms with high computational speed, low grid dependence, and high accuracy of results. Meanwhile, the thin water film and large deformation of the stern bearing bring great difficulties to modeling, meshing, and boundary conditions setting of computational fluid dynamics (CFD) calculations. Thus, it is necessary to strengthen the scientific and reproducibility in the coupled thermo-hydro-solid analysis of WLSBs [2].

2.2 Simulation of WLBs characteristics

The research of WLBs mainly focuses on their characteristics of lubrication, loading, and dynamic performance. The parameters of its structures and materials directly determine the performance of WLBs as internal factors, while the effects of in-use conditions and environments cause the change in service life. This section would review the evolution mechanism of WLBs through the simulation studies.

Numerical analysis and finite element analysis were usually used to simulate the characteristics of WLBs. The numerical analysis method was suitable for the calculation of loading capacity and liquid film characteristics with high precision, but with low calculation efficiency and poor adaptability to complex structures. The finite element method could be used to analyze the lubrication characteristics with better

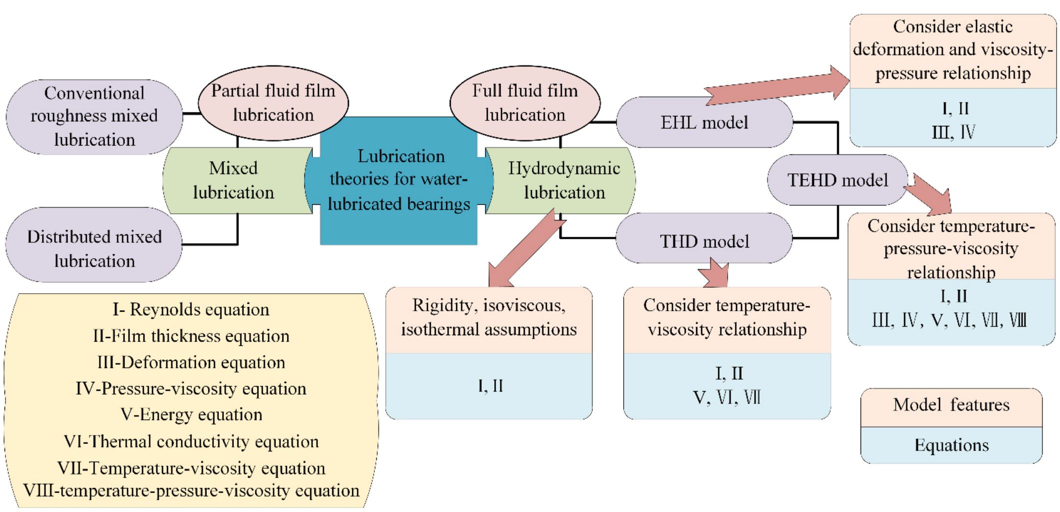

Fig. 5 Lubrication theories for WLBs.

Table 2 Model and solution methods for lubrication of WLBs.

Model		Features	Boundary conditions & solution methods	Researchers
HD model	Infinite length bearing theory	Constant, $l \gg d$; no axial flow, pressure uniformly distributed along the axial direction	Reynolds condition	Sommefeld [4]
	Short bearing theory	Constant, $l \ll d$; neglecting the axial pressure flow	Sommefeld or half-Sommefeld condition	Ocvirk [5]; Dousti [7]
	Finite length bearing theory	Constant	Galerkin method; Small parameter expansion method; FEM; Difference method [6]	Majumdar et al. [6]; Dousti [8]
EHL model	Conventional EHL	Consider elastic deformation of bearing material	Finite element method [9]. EHL+LW model [10]. Red-black successive over-relaxation method [11]	Tang et al. [9]; Wojciech Litwin [10]; Shi et al. [11]
	SEHL	Large deformation of the shaft pad material	/	Hooke et al. [12, 14]; Huang et al. [13]
THD model		Adiabatic flow assumption	'Effective temperature' method; CFD	Wilcock [15]; Xi'an Jiaotong University [17]
		Consider heat dissipation by thermal conduction	FDM [18]	Dowson [16]
TEHD model	Conventional TEHD	/	FDM; FEM [43, 44]; FDM-FEM; CFD-FEM [21, 45]	Sternlicht et al. [46]; Liang et al. [45]
	TSEHD	/	/	/
ML model	Conventional roughness ML	Roughness statistical model or deterministic model	Multi-level integration method [47]; FFT-multiple mesh method [39]; DC-FFT [48, 49]; Linear perturbation method [50]; FDM [40]; AICV*+DFFT[51]; Herringbone mesh difference method [40]; Local adaptive FEM [52]	Jiang et al. [39]; Han et al. [40]; Liu et al. [48, 49]
	Distributed ML	Consider lubrication partition and distribution characteristics	Computational strategies for decomposition and synthesis	Ouyang [41]

Notes: *AICV: asymmetric integrated control volume discretization scheme.

adaptability to complex structures and higher computational efficiency. However, it has poor adaptability to multi-structure and multi-working conditions. To analyze the performance of WLBs more comprehensively, these two methods are generally combined [54]. A review of the simulation studies for different WLBs is shown in Table 3.

As shown in Table 3, the studies of WLBs simulation have covered all types (e.g., stable and transient, cavitation and non-cavitation, laminar and turbulent flow, alignment and misalignment, textured and non-textured, etc.) to simulate the lubrication, loading, and dynamic characteristics. It should also be noted that the study of dynamic characteristics needs to consider the coupling relationship with the shaft system.

This section reviewed the research on lubrication theory and characteristics simulation of WLBs. The models of hydrodynamic lubrication and mixed lubrication and their algorithms were compared to summarize the advantages and disadvantages of each model, and some possible improvement directions were proposed.

Table 3 A review of simulation studies on the characteristics of different WLBs.

Bearing types	Working conditions/objects	Methods or models	Results	Ref.
Sliding bearings	Start-up process	Dynamic mesh technology	Pressure and velocity distributions	[55]
	Shutdown process	Transient kinetic analysis (Abaqus/Standard)	Effect of specific pressure and friction coefficient on vibration	[56]
	Pure, salt, and sand water	FSC* numerical simulation	Water film pressure, load surface deformation, and stress changes	[57]
	Material parameters, speed, and load	Bidirectional FSC algorithm	Maximum water film pressure, minimum water film thickness, friction factor, etc.	[58]
	Shaft inclination and eccentricity	CFD simulation	Pressure distribution and fluid flow state	[59]
	Operation parameters such as speed and load	FDM + boundary conditions from experiments	Evolution mechanism of temperature field	[60]
	Large L/D** and shaft bending	FSC model	Lubrication performance distribution and optimization directions	[61]
	Aligned and unaligned conditions	FSH model*** with a shaft deflection model	FSH performance	[62]
	Dynamic wear	Modified Archard model + transient mixed EHL model	Evolution of wear and mixed EHL performance distributions over time	[63]
	Misaligned and edge wear	Modified Archard model + PC Flow Model	Validation of profile design method for edge wear reduction	[64]
	Texture bottom shape & ML	Lubrication gap equation with wear depth distribution	Transient interaction between wear and ML	[65]
	3D thermal effect and non-linear external shock	Numerical model	Transient frictional dynamics response & local groove design scheme	[66]
	Localized wall slip	Reynolds equation was extended by the ultimate shear stress model	Interaction between wall slip and the hydrodynamic characteristics	[67]
Coupled micro-groove journal-thrust bearings	Coupling effects and different groove structures	Numerical model	Loading capacity and lubrication performance	[68]
	Positive and negative misalignment modes	The transient dynamics model considering the axial micro-vibration	Transient lubrication performance	[69]
Tiltable tile journal bearings	Multiphase flow, thermal-fluid, transitional turbulence, and thermal deformation	3D FSC based on FSI-CFD****	Static response of the journal and pads in a non-vibration state	[70]
		CFD-FEM	Dynamic response of bearing stiffness and damping	[71]
	Multimodal lining flexibility effect	Advanced mixing prediction method for BP thermal flow based on FSI-CFD	Prediction accuracy of static and dynamic performance improved	[72]
		Neural network deep learning method	CFD model computational efficiency improved	[73]
Thrust bearings	Elastic modulus and eccentricity rates	3D FSI-CFD model considering cavitation and lining deformation	Stiffness coefficient of the water film	[74]
	Polymer-coated gasket rubber pads	TEHD model	Optimum eccentricity ratio	[45]
	Rotor-bearing system transient model of RDT	Rubber damping is characterized by damping loss factors	External excitation on the lubrication performance	[75]
	Texture parameters and cavitation effects	Numerical model	Loading capacity and friction characteristics	[76]
	Groove parameters and speed	Turbulent Reynolds equation combined with the JFO cavitation model	Static performance, complementary to the traditional laminar flow model	[77]

Notes: *FSC: fluid-solid coupling; **L/D: length-to-diameter ratio; ***FSH: fluid-solid-heat coupling; ****FSI-CFD: fluid-structure interaction computational fluid dynamics.

3 Performance test techniques for WLBs

It is an effective method to measure and evaluate the performance of WLBs by parameters from the WLBs performance test. This section would review the typical WLBs test devices and parameter identification methods.

3.1 Test devices of WLBs

As shown in Fig. 6, according to the different objects, WLBs test devices could be classified into three types just like basic tribological test, bearing model test, and appraisal test.

The basic tribological properties test devices for specimen could perform different types of friction tests on specimens such as rotations, reciprocating, block on ring drive, micro-movement, scratching, and high-speed long stroke. It is necessary for WLBs to consider the corrosion of water on metals and the simulation of the sediment environment, so the basic tribological test devices of test block are generally customized, such as the ring-block test device [78], ring-plate test device [79], etc. These devices could simulate different operating conditions by changing the frictional wear method and time, motor speed, test environment, and preload force on the specimen. The friction coefficient of the specimen could be calculated by friction force. The surface morphology information of the specimen could be identified by scanning electron microscope (SEM), atomic force microscope (AFM), or X-ray diffraction (XRD) after the test to analyze the basic tribological properties such as the wear state [80] and stick-slip phenomenon of the materials [81].

The model test is used to acquire the performance test of shrinkage bearings or full-size bearings [42], the appraisal test device [82] is used to simulate the real-life condition of a real propulsion shaft system and evaluate whether the bearing meets the design requirements. According to different loading methods, the radial bearing test device could be divided into positive [83] and inverted types. The load of the positive is located on the shafts on both sides of the test bearing with a downward direction, which could simulate bias load. The load of the inverted acts on the test bearing in an upward direction. The thrust bearing test device could be divided into vertical and horizontal types according to the structure form. Compared with the horizontal, the vertical is simpler because the lubrication seal structure is cancelled.

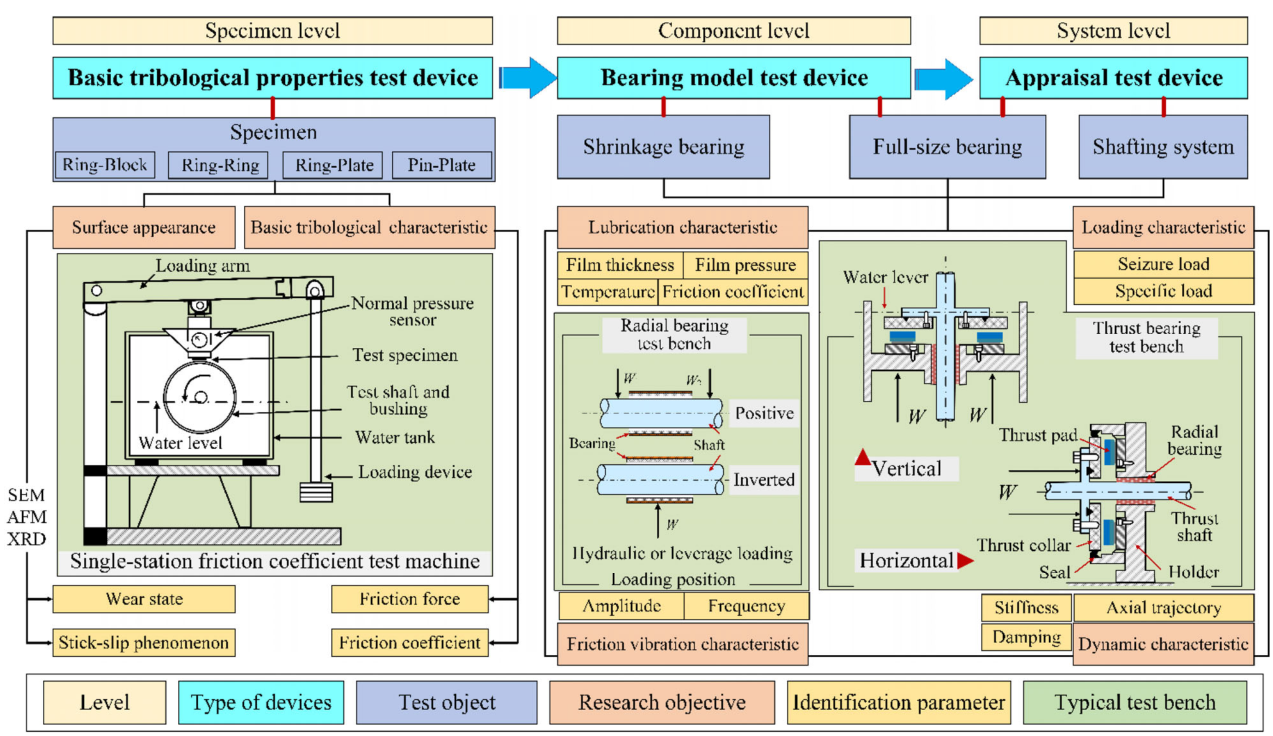

Fig. 6 Test devices and performance tests of WLBs.

By considering the example of the water-lubricated test rigs built by the Wuhan University of Technology, the corresponding information and pictures are shown in Table 4 and Fig. 7.

3.2 Parameter identification methods

The WLBs performance could be determined by the water film quality, including pressure distribution, temperature, film thickness distribution, and kinetic parameters. An overview of the identifications for WLBs lubrication water film is shown in Table 5.

In this paper, the difficulty level of the test methods is comprehensively evaluated by the maturity of the sensor itself, the universality of use in the field of water/oil lubricated bearings, test accuracy, test environment, technical maturity (such as test principle, laboratory verification and practical application, etc.), and the number of literature reports. The difficulty level of the test method is considered to be lower when the method has the characteristics of the more mature sensor, the wider application in related fields, the lower test environment requirements, the more literature reports, the simpler test principle, and the more reliable verification test method. In Table 5, the difficulty level is represented by the number of ★, and the difficulty level is positively correlated with the number of ★.

As shown in Table 5, the measurements for

Table 4 Information of the bearing test rigs of the Wuhan University of Technology.

Types	Driving module	Loading module	Lubrication module	Functions and possible studies
(a) Vertical journal-thrust bearing test ring [84]		» Hydraulic loading » Radial and axial loading » Static and dynamic loading	» Water lubrication » Heating function » 0–60 L/min	» Load-bearing mechanism; » Structural modification of thrust bearings; » Wear life prediction of radial bearings; » Dynamic behavior of combined radial-thrust bearings; » Frictional vibration mechanism and vibration reduction measures
(b) Inverted stern bearing test ring (SSB-200)		» Hydraulic loading » Radial loading » Intermediate loading		Water lubricated stern bearings (WLSBs): » Fault diagnosis analysis [85]; » Loading mechanism; » Mechanism of vibration squeal generation and suppression
(c) Horizontal thrust bearing test ring [45]	Frequency conversion motor	» Radial loading	Water lubrication	» Thrust bearings; » Loading mechanism and take-off characteristics [86]; » Observation of lubrication state transitions [87]; » Static and dynamic characteristics tests
(d) Ship shafting dynamic characteristic system		» Hydraulic loading » Radial and axial loading » Static and dynamic loading		1) Hull deformation excitation [88]: » Vibration characteristics of the shaft system; » Forces analysis of the shaft system; 2) Multiple excitations: » Shaft system dynamics analysis [83, 89]; » Shaft system vibration control methods
(e) Testing platform for shafting system [90]		» Hydraulic loading » Three directional loading	» Water lubrication (rear stern bearing) » Oil lubrication (front stern bearing)	» Effect of shocks on shaft transmissions; » Lubrication mechanism, structural improvement and material selection of WLSBs; » Mechanical seals; » Monitoring methods, safety evaluation, and maintenance of shaft systems; » Shaft alignment and vibration and noise reduction in shaft systems [91]

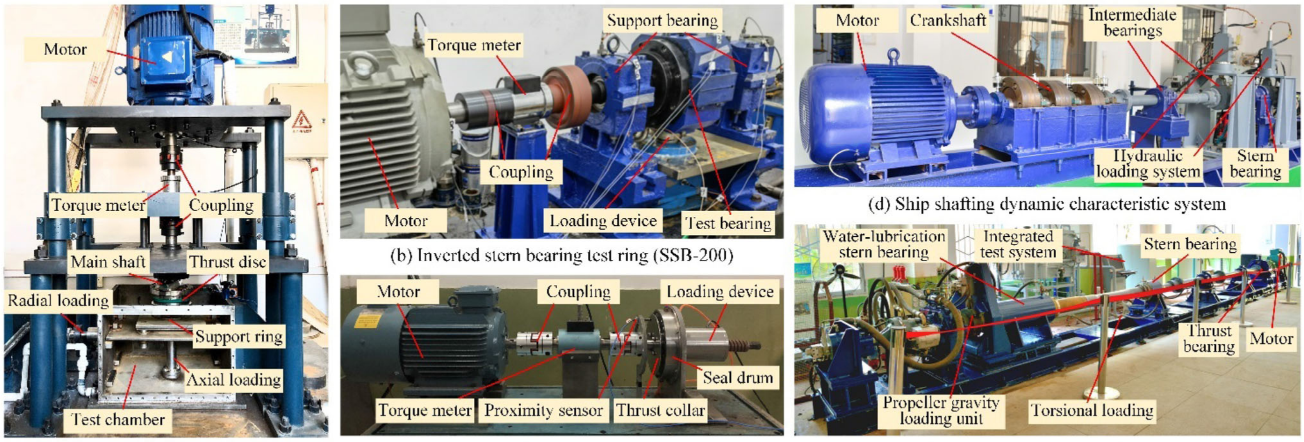

(a) Vertical journal-thrust bearing test ring (c) Horizontal thrust bearing test ring (e) Testing platform for shafting system

Fig. 7 WLBs test rigs of Wuhan University of Technology.

vibration, temperature, and pressure have been quite developed to meet the requirements of various tests. However, it is difficult to measure the film thickness and the distribution of all performance parameters, which are closer to the characteristic parameters of bearing service and more directly reflect the bearing performance. In addition, the *in-situ* measurement of wear is also a challenge. The stiffness and damping identification of WLBs is derived from the measured values of force and displacement, which belongs to indirect measurement with low accuracy and large error.

This section focused on the performance test technology and test device of WLBs, and summarized the characteristics of different test technologies and devices. It is a great challenge to realize the distributed and online test of WLBs performance and improve its test accuracy.

4 Friction-reduction technologies for WLBs

The marine WLBs are easily under the mixed lubrication. Especially, in certain extreme conditions such as the start/stop phase or at low speed and heavy load, the bearings are easy to suffer from the boundary lubrication or even a dry friction state. It would reduce the efficiency of the shaft system and cause serious wear, or even threaten the safety of the ships.

To achieve the WLBs' friction reduction, bearing design and material selection should be carried out to avoid the bearings working in poor lubrication. This section would review the research and application of friction-reduction technologies for WLBs from two aspects: structural optimization and material modification.

4.1 Structural optimization

Structural optimization could improve the tribological properties of bearings by optimizing the structural form or applying the appropriate surface treatment. The optimization research of basic structures (e.g., the L/D, clearance, and groove structure, etc.) [130–135] has shown that the structural parameters interact with each other to jointly influence the bearing performance. In addition, the lining structure of WLBs could be divided into integral type and slab type [2]. The surface type of slab bearing (such as flat type, concave type, and convex type) would affect the bearing performance [78, 136]. Therefore, it is essential to perform multi-factor coupled optimization [137] and synergistic optimization with operating parameters [138] when bearing is designed.

This section would review the friction-reduction applications of surface texture techniques and magneto-hydraulic composite structures on WLBs.

4.1.1 *Surface texture*

Surface texture is fabricated by precision machining techniques to form different morphologies such as pits, grooves, or micro-convex on the friction surface and improve the tribological properties. As shown in Table 6, a series of researches on surface texture has been carried out by the Wuhan University of

Table 5 Test methods for water film properties.

Characteristic	Parameters	Test methods	Realization methods	Objects/effects	Notes	Difficulty level
Lubrication characteristic	Pressure	Sensors installed on the test bearing [92]	SPP* sensors based on MEMS [6, 93–95]; FBG sensors [96, 97]; PDMS sensors[98];	Pressure variations at several fixed points	Pressure sensors	★★
		Sensors installed on the shaft [61, 82, 99];		Continuous pressure distribution along the circumferential direction		★★★
		Bearing lining covered by sensors array	New piezoelectric material — **EMFi or PVDF [100–103]	Full-bearing water film pressure distribution [104]		★★★★★
	Temperature	Contact measurement	Thermocouple temperature sensor	The temperature at inlet and outlet pipes [92], inside the lubrication tank [105], or on the inning surfaces [106]	Analyze the temperature rise of the water film	★
			Fiber grating [107, 108]			★★
		Non-contact measurement	Infrared temperature measurement principle [109]	Temperature monitoring of bearing shells	Less application	★★
			Spectroscopic analysis of CeTe quantum dots films [110]	The temperature inside the bearing	Not applied to water film of WLBs	★★★★
	Film thickness	Electricity	Resistance method [110]	Presence or absence of lubricating film	Easy to install and measure, but accuracy is not high	★
			Capacitive method [111]	Average film thickness		★★
			Eddy current method [112–114]	Minimum film thickness		★★
		Magnetic	Resistive oscillation method	Average film thickness	Produce thermal effects	★★
			Magneto-resistive method	Minimum film thickness		★★★
			Magnetic fluid methods [115]	Film thickness at a contact point or small area		★★★
		Optics	LIF*** method [116-119]	Thickness distribution in contact area by advanced LIF model [117]	High calibration and installation requirements, high accuracy	★★★★
			Reflected light intensity method	Average film thickness		★★★★
			Optical interferometry [120, 121]	Lubricant film shape		★★★★
			Optical fiber displacement sensor method [122, 123]	Minimum film thickness		★★★★
			Laser displacement sensor method [124]	No results provided		★★★★
			Raman spectroscopy [125]	Film thickness at a contact point or small area		★★★★
		Sonic	Ultrasonic method	Average film thickness	Non-destructive testing	★★★★
			Reflection coefficient method	Average film thickness	Acoustic attenuation	★★★★

(Continued)

Characteristic	Parameters	Test methods	Realization methods	Objects/effects	Notes	Difficulty level
Wear	*In-situ* test	Weight-check	/	Wear mass	Off-line monitoring	★
	Non-*in-situ* test	Same as the film thickness test method based on sonic		Wear depth	Online monitoring	★★★★★
Dynamic properties	Stiffness and damping	External excitation device [83]	Vertical excitation method	/	Small horizontal amplitude response	★★
			Cross excitation method		More accurate identification results	★★★
		Without excitation device	Time-domain multi-conditions method	Good repeatability, large size radial sliding bearing	E.g., disturb the initial phase method [126]	★★
			Unbalanced response identification method [127–129]	Based on the rotor-bearing system	Change the dynamic balance	★★

Notes: *SPP: silicon piezoresistive pressure; MEMS: micro-electromechanical systems; FBG: fiber Bragg grating; PDMS: polydimethylsiloxane; **EMFi: Electromechanical Film; PVDF: polyvinylidene fluoride; ***LIF: laser-induced fluorescence.

Table 6 Researches on surface texture at Wuhan University of Technology.

Objects	Research contents	Results	Ref.
Local texture; oil-lubricated	Position and dimple depth	The theoretical basis for the dimple texture design	[139]
EHL model; micro-groove	Eccentricity ratio and material	Optimal texture depth for different materials	[140]
Three pit textures	Surface texture flow field	Decreasing average velocity; least water film pressure with inclined cylinder pit texture	[141]
Three micro-convex textures	Experiment; tribological performance; enhancement mechanism	The most stable dynamic friction performance of cylindrical structure; more suitable for low-speed conditions of the cube structure	[142]
UHMWPE materials with three Koch snowflake textures		Gradient effect on water film pressure to lead to greater improvement of composite texture	[143]
TPU samples with 12 types of spherical-convex texture		Wedge-shaped gaps formed by textures facilitate the hydrodynamic lubrication; 1/3 spherical texture with surface density of S= 38% is better.	[144]
TPU; diamond-shaped textures with different heights/depths		Producing converge and cavitation effects and preventing the accumulation of abrasive particles; 1mm convex is the best.	[145]
HDPE with 9 spherical platform textures		Promote wedge and lubrication cavitation effects; a 1/2 spherical platform and a 1mm top surface diameter is better.	[146]

Technology. Among them, the basic tribology studies on texture types of Guo et al. are shown in Fig. 8.

The studies indicate that surface textures enhance the performance of wedge-shaped gaps or local stepped structures between contact surfaces to improve the effects of the wedge, converge, and cavitation or pressure gradient [146]. These effects would promote the formation of hydrodynamic lubrication to reduce the adhesive effect and prevent the accumulation of abrasive particles [145]. Surface textures could significantly enhance the level of fluid lubrication to improve the tribological characteristics of WLBs by designing the correct form and setting appropriate locations [139].

To resolve slow computing rate and limited computing scale of the traditional numerical methods for multiscale surface texture hydrodynamic lubrication, the finite cell method (FCM) was proposed by Pei

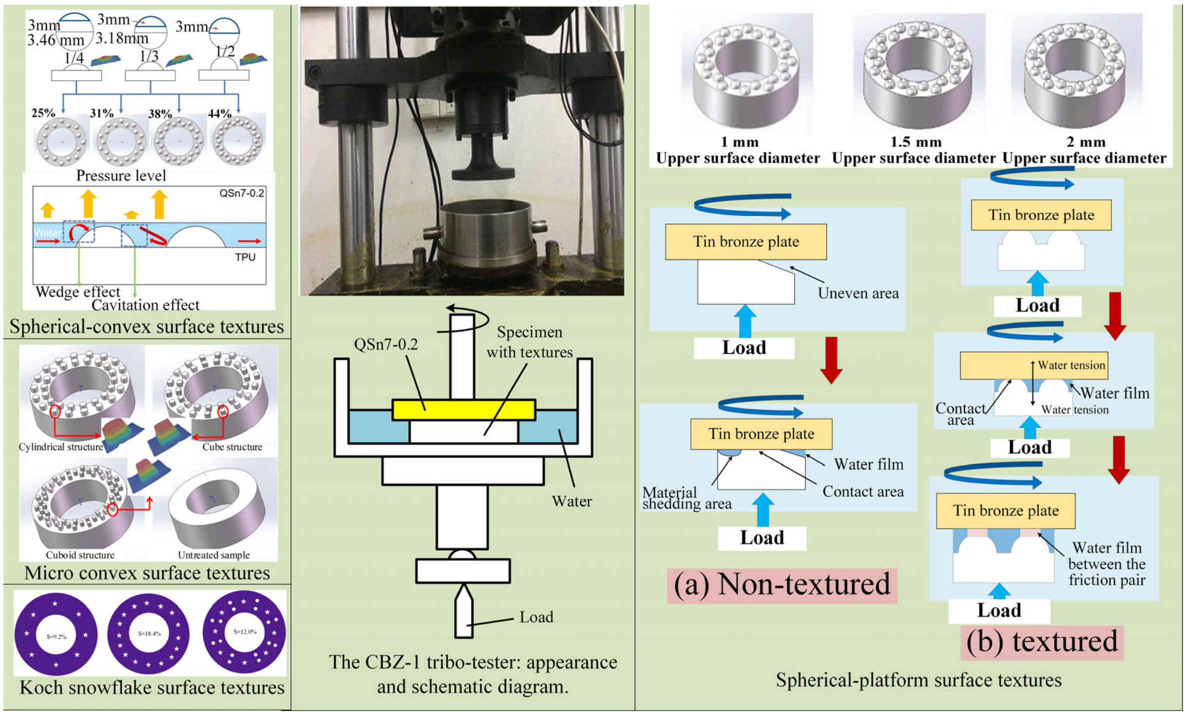

Fig. 8 Studies on the surface textures. Reproduced with permission from Refs. [142–144], © Elsevier 2019; Ref. [146], © Elsevier 2021.

et al., which was proved to significantly improve solution efficiency of large-scale texture [147]. This method is successfully applied to solve the problem of the static and dynamic performances of oil lubricated offset bearing with surface texture [148], and further improved to improve robustness and computational efficiency [149]. The FCM and its derivative method can be employed for the simulation study of WLBs with surface texture.

4.1.2 *Magneto-hydraulic double-suspension bearings*

The magneto-hydraulic double-suspension bearing technology combines the advantages of liquid hydrostatic/dynamic pressure and magnetic suspension. This structure can play a role of magnetic force loading at low speed, and the joint loading of magnetic and hydraulic force at high speed to prevent frictional surfaces from contact. Therefore, it could reduce friction, improve operational stability, and increase loading capacity.

Figure 9 illustrates the application of magneto-hydraulic double-suspension technology for bearings. One of the important was the artificial blood pump [150]. Elsewhere, this technology was used to improve start/stop characteristics [151], dynamic performance [152], or as a maintenance-free solution [153], etc., but some designs were unsuitable for marine WLBs because of their application scenarios [154, 155] or structural forms [156]. Ouyang et al. introduced it to the applications of water-lubricated thrust bearings [157] and radial bearings with the permanent magnets adopted and proposed the fixed/tilting pad thrust bearings and high-load radial bearings with magneto-hydraulic double-suspension structure [158, 159].

It is beneficial for WLBs to employ magneto-hydraulic double-suspension technology because it could improve their friction-reduction performance, loading capacity, and operational stability. However, the current research exhibits unclear mechanisms of multi-physical fields coupled and weak proactive design ability. It is necessary for magnetic coupling structure to explore its internal synergistic evolution mechanism between bearing force and deformation in thermal-fluid-solid-magnetic multi-physical fields.

4.2 Material modification

The structural optimization could enhance the formation

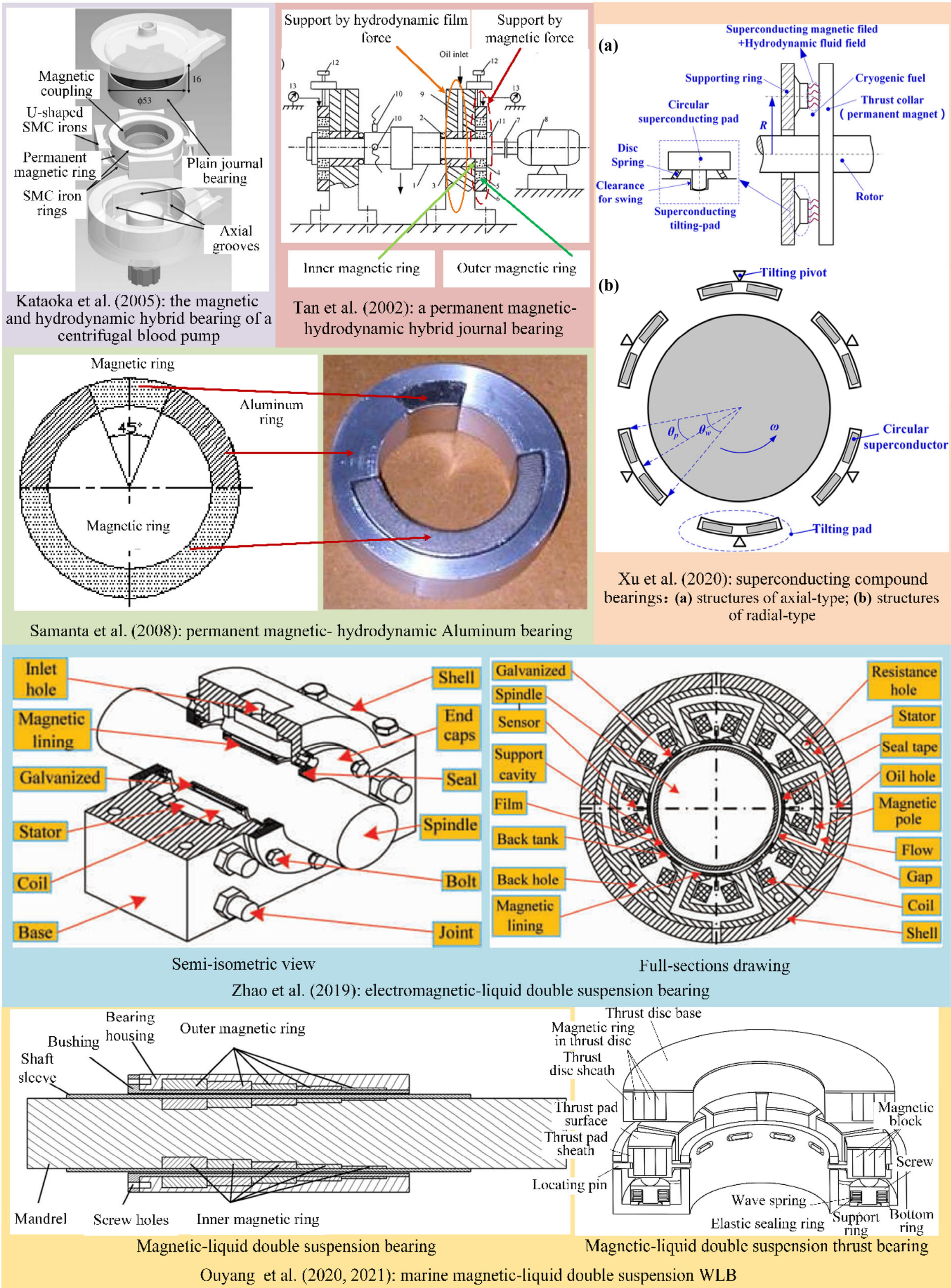

Fig. 9 Application of magneto-hydraulic double-suspension technology for bearings. Reproduced with permission from Ref. [150], © John Wiley and Sons 2005; Ref. [151], © Elsevier 2002; Ref. [152], © IEEE 2008.

and retention ability of the lubrication water film to reduce the contact of the friction interface. However, under specific conditions such as the bias load or at start/stop phase and low-speed heavy-load, the inevitable frictional surface contact would result in boundary lubrication or even dry friction which could cause an increased friction coefficient. Therefore, it is necessary to modify the bearing materials to improve the lubrication capacity when contact occurs.

4.2.1 Blending modification

The blending modification of friction reduction employs a more stable interlayer to functionate as stable self-lubrication and separate the contact surfaces [160]. The formation mechanism of the interlayer has been explained and classified in detail, which involved the friction process caused by mechanical, physical, or chemical effects [161]. Moreover, the synergistic lubrication phenomenon of the interlayer has been observed by the other studies [162–166].

As a widely used WLBs material, nitrile butadiene rubber (NBR) has been a great concern for material modification to improve its tribological properties. Zhou et al. modified NBR by blending MoS_2 nanoparticles [164], UHMWPE and graphene powder [167], and SiO_2 [168] or nano-SiO_2 [169] to obtain good friction properties at a low speed. Qu et al. [170] blended polyurethane (PU) and epoxy (EP) into NBR to produce novel ternary NBR/PU/EP interpenetrating polymer networks (IPNs) and obtained a minimum friction coefficient lower 75.4% than that of pure NBR. Blending modification with suitable material could provide a better friction-reduction effect for NBR.

More and more polymer materials have been used for marine WLBs to improve their performance. To reduce the friction of these materials, scholars began to pay attention to the research on material modification. Figure 10 shows the blending modification of polymer materials. Figure 10(a) is the direct blending modification with a different mechanism. The ① is the utilization of micro-convexity and rolling formed by particles [164, 168, 169]; the ② is by reducing the material hardness and increasing the load bearing area [170]; the ③ is the weakening of deformation and sticking [80, 171–173]; and the ④ is the promotion of water-film formation by the hydrophilic/absorbent nature of the materials [174–177]. But it may be difficult for direct blending to achieve an ideal lubrication effect due to the material compatibility limitation. In this case, the self-lubricated microcapsule structure as shown in Fig. 10(b) could be considered for material modification [178, 179]. The urea-formaldehyde resin

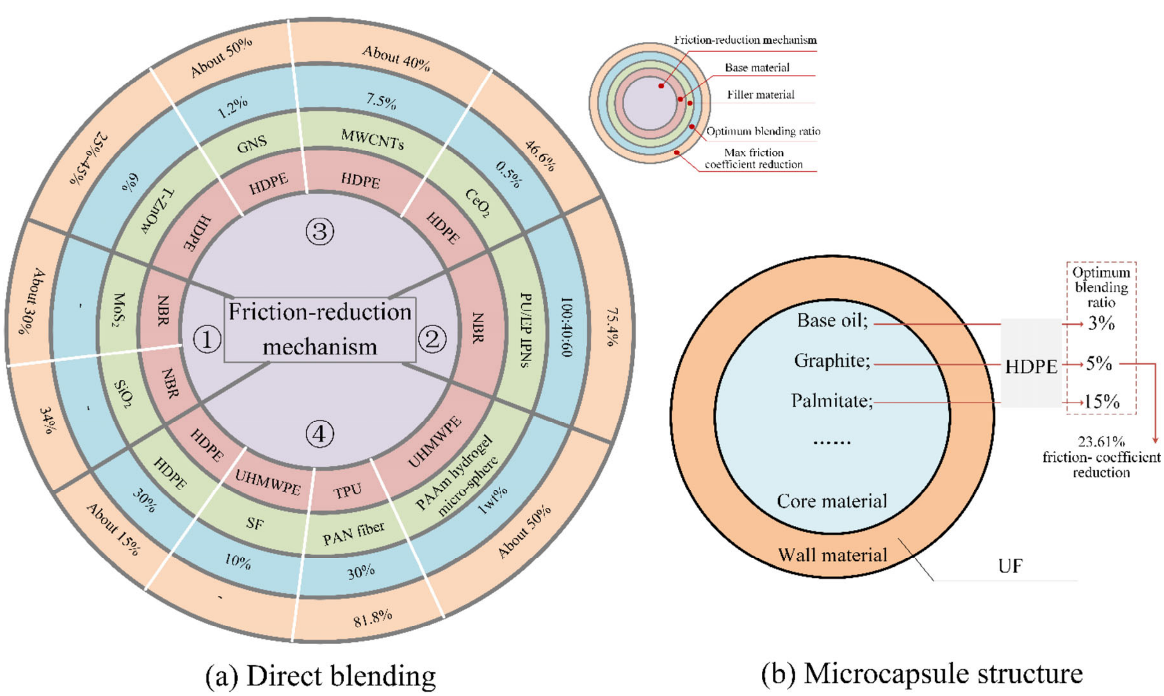

Fig. 10 The blending modification of polymer materials: cases and mechanism.

(UF) is always used as the wall material, the base oil [178], graphite [179], and palmitate [180] could be used as core material to constitute the microcapsule structure.

4.2.2 Bionic modifications

It is greatly significant for the achievement of ships' green friction goal to apply bionic principles and design materials with self-lubricated structures to develop new WLBs with low friction factor, high loading capacity, low noise, and good self-lubrication performance. Guaiac resin as oily resin could promote the formation of lubrication water film and thus improve the friction and wear properties of the material [181]. Guo et al. prepared the HDPE/guaiacum to reduce the friction coefficient of the material, which was a self-lubrication bionic material referred to the composition and surface structure of lignum vitae [182] and lignin [183]. The self-lubrication microcapsules shown in Fig. 10(b) are also bionic applications for the structure of lignum vitae.

In addition, some researchers have also focused on the surface morphology of snakes [184] and water snail [185] etc., to develop surface textures with similar structures to reduce friction. Human joints have excellent lubrication and a very low friction coefficient at high loads [186]. This superior interfacial lubrication mechanism is also a major research topic in bionic water lubrication. The skin of earthworm exhibits low friction characteristics when it moves in the soil. This low friction is not only from the annular micro-groove structure on the skin surface of earthworms [187] but also from the coupling effect of surface structure and interfacial lubrication [188, 189]. The review of Li et al. [190] illustrated the bionic modifications in WLBs more systematically and enumerated several preparation methods of typical materials or structures. Bionic modification is expected to promote the performance of WLBs.

4.2.3 Ion implantation

The friction pairs of WLBs are mainly made of metal, ceramic, and polymer materials. Ion implantation is an advanced technique to modify these materials' surface properties without changing the original properties of the matrix material [191]. This technology can obtain a high alloy concentration on the surface of the material only by injecting a small amount of alloy elements, thereby effectively improving the wear resistance, corrosion resistance, oxidation resistance, and fatigue resistance of the material surface [192, 193]. The studies on surface modification of metal materials [194, 195], ceramic materials [192], and polymer [193] by ion implantation technology indicate that it can effectively improve the wear resistance and surface hardness of matrix materials, and the friction coefficient of some materials also decreases. Ion implantation has great application potential in the field of WLBs.

Currently, ion implantation has been widely used in the fields of photovoltaic materials [191], electronic devices [196], and medical devices [195], but research or application in the field of WLBs has not yet been seen. The specific effects of ion implantation on the performance of WLBs need to be explored by combining the materials and application conditions of WLBs to further guide the practical applications.

5 Wear mechanism and wear resistance technology for WLBs

It is significant for service performance enhancement of ships to improve the WLBs wear resistance because of its great influence on operational performance and the service life of WLBs. This section would overview the influencing factors of WLBs wear from wear mechanism and review the wear resistance enhancement methods from material modification and friction matching pairs optimization.

5.1 Wear mechanism

It is important for WLBs wear research to reveal the mechanism of wear failure and propose available life prediction methods. Liu et al. [197] summarized the failure forms of water-lubricated radial bearings and found that most of the rubber bearing failures were related to wear.

5.1.1 Main wear forms of WLBs

Adhesion wear is a major wear form of marine rubber stern bearings. Drummond et al. [198] explained most stick-slip friction by the model based on the kinetics of formation and fracture of adhesion between two sheared surfaces. Furtherly, an improved model of the stick-slip friction was proposed [199, 200]. Dong et al. [201, 202] revealed the adhesion wear mechanism of NBR by pin-disc test and pointed out that severe adhesion tearing wear occurred between the friction pairs under water lubrication conditions. This wear process was a cyclic process of adhesion – stretched or deformed – tearing – re-adhesion – stretched again – tearing again. Moreover, high lubricating water temperature in some extreme conditions could lead to a separation of some composite components (such as the polymer resin (PR) substrate component) to cause strong adhesion wear [203].

Abrasive wear is another major form of WLBs mechanical wear. It usually occurs in open-type WLBs working in turbid water by the influence of sediment or hard suspensions. In this process, the hard particles wear the bearing surface and produce microforms such as grooves, scratches, and impact pits through the impact, shoveling, plowing, and cutting action. The hard particles with appropriate particle size [204] would destroy the water film and retain in the friction pairs [205] to exacerbate the wear process. Zhou et al. [206] obtained similar conclusions and the main wear mechanisms were shown in Fig. 11. The research pointed out that the sediments entering the WLBs would mainly result in furrow wear, but clay might reduce the wear because it might adhere to the surface of the friction pairs to prevent direct contact and convert particle-NBR wear into clay-NBR wear.

Adhesive wear and abrasive wear would occur simultaneously and abrasive particles formed by adhesive wear could cause abrasive wear [201]. During the friction process, when the load is too large and the interface heat dissipation is insufficient, the surface of the friction pair of the metal-polymer material would adhere, and the metal protrusion would be torn off and embedded into the surface of the polymer material. After further friction, the metal abrasive particles embedded in the surface of the polymer material would appear hardening effect, and then grinding with the metal surface of the friction pair like "sandpaper". Two-body abrasive wear is converted into three-body abrasive wear [207], forming a so-called "soft wear hard".

Concurrent multiple forms of wear could cause complex interactions. Ning et al. [208] analyzed the worn surface morphological characteristics of the Aluminum bronze (ZCuAl9Mn2)/PEEK friction pairs. Then, the wear evolution mechanism was proposed as shown in Fig. 12 by considering the effects of frictional heat effect and oxidative decomposition on wear based on adhesion and abrasive wear. It involved the process of contact-adhesion-thermal expansion-thermal oxidative decomposition-avulsion-plowing.

5.1.2 *Influence factors of bearing wear*

(1) Influence of friction pairs hardness on bearing wear

Liang et al. observed the worn microscopic

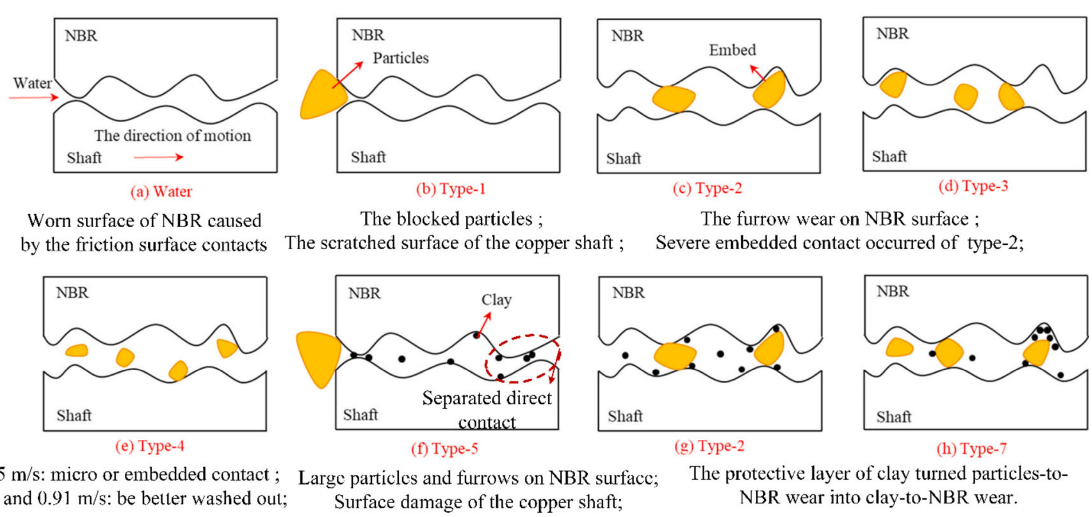

Fig. 11 Mechanisms of the effect of sediments on NBR wear. Reproduced with permission from Ref. [206], © Elsevier 2021.

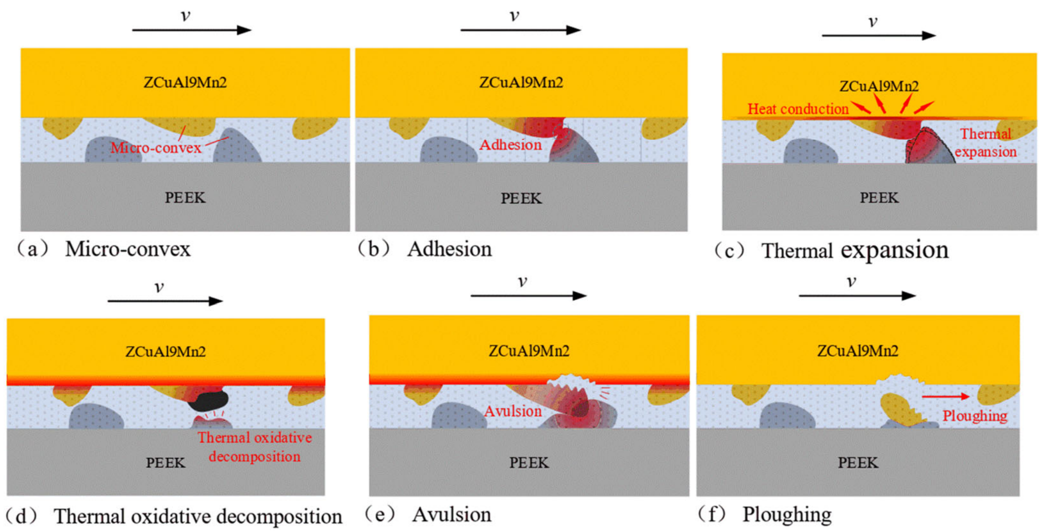

Fig. 12 Wear evolution mechanism of water-lubricated ZCuAl9Mn2/PEEK friction pairs. Reproduced with permission from Ref. [208], © IEEE 2021.

morphology of the thrust ring with aluminum bronze/Throden SXL friction pairs [86] and compared the wear results with stainless steel/PEEK friction pairs [209], which concluded that harder frictional subsets could increase the loading capacity of thrust bearings and reduce wear. Therefore, six sets of friction pairs with different hardness combinations as shown in Table 7 were tested and the results indicated that the increasing hardness of thrust rings would reduce the production possibility of abrasive particles and improve wear resistance [207].

(2) Influence of operation conditions on bearing wear

The speed and load could significantly influence the wear process of WLBs. The water-lubricated NBR pin-disc tests observed a large number of spalling particles at low-speed operation and a lot of tiny pits and particles at high-speed operation. The wear increased dramatically when the load increased [202].

Material aging which is caused by increasing temperature would lead to performance degradation of friction and wear. The rubber is sensitive to temperature that the increasing temperature would significantly reduce its mechanical property and further affect its tribological property [210]. Frictional heat may lead to a temperature rise of 5–10 °C on

Table 7 The effect of hardness on friction pairs wear.

Bearing
inner diameters=40 mm;
outer diameters =90 mm;
pad angle=41.4°;
thickness=9 mm;
		Thrust collars
		inner diameters=36 mm;
		outer diameters =120 mm;
		thickness=7 mm
				Load	Wear results	Wear conditions

Material	Hardness	Material	Hardness			
PEEK	Shore D90	Aluminum bronze	<19 HRC	1,600 N & 2,600 N	WRB=37.5/1033.5 μm/h (1,600 N/2,600 N)	Severe adhesive wear and abrasive wear
		3Cr17NiMo	53 HRC		DWF ≈10 μm	Stable running state
		Si_3N_4	89 HRC		Slight wear	Stable running state
Polyurethane	Shore D67	Aluminum bronze	<19 HRC		WRB=3.5/6 μm/h; DWF >40 μm;	Running in
		3Cr17NiMo	53 HRC		DWF ≈10 μm	Stable running state
		Si_3N_4	89 HRC		Slight wear	Stable running state

Notes: WRB means the wear rate of the bearing; DWF means the deepest wear furrows on the thrust collar.

the wear surface compared with the environment due to the extremely poor heat dissipation properties of rubber [202]. It would further aggravate the temperature rise of the rubber bearing because of the surface contact under heavy load, low speed, and muddy water conditions [211]. Marine stern bearings are required to operate constantly for a long time, which would accelerate the rubber aging. The NBR-pins under different accelerated aging times indicated that the resistance to fracture and tearing of NBR decreased sharply when the large cracks and wear particles formed due to a certain degree of aging, which further led to a decrease in wear resistance [212].

In summary, the lubrication conditions, load, and speed change the frictional wear state by influencing the adhesion and hysteresis friction of the friction pairs which further affect the service performance of the bearing. Service safety needs to assess the reliability life of bearings. Dong et al. fitted the material wear test data to obtain 1) an equation for the wear of NBR as a function of mechanical parameters, load, and speed [201] as shown in Eq. (1), and 2) an empirical equation for the volumetric wear of NBR under pure water lubrication [202] as shown in Eq. (2):

$$A = 2.227 \times 10^{-4} H^{1.0133} N^{0.7876} v^{0.5499} \quad (1)$$

$$V_X = \frac{V}{L} = \frac{4.35 \times v^{-0.6505} N^{0.8193}}{\left\{30 \exp\left[-183510 \exp\left(\frac{-5186.35}{T}\right) t^{0.52}\right]\right\}^{1.191}} \quad (2)$$

where A is the wear mass loss rate (mg/h), H is the shore hardness of the NBR (A), N is the load (MPa), and v is the velocity (m/h); V_X is the average stroke wear volume (mm^3/km), V is the wear volume (mm^3), L is the sliding distance of stainless steel plate on NBR (km), t is the aging time (d), and T is the aging temperature (K). The prediction error of Eq. (1) is basically below 10% and could be applied in engineering practice.

5.2 Methods for wear resistance enhancement

It is possible to improve the wear resistance of bearings from both structures and materials. Structural modifications are similar to the groove design and surface texture [213] methods used in Section 4 for friction reduction, which aims to promote the formation and maintenance of lubricating water films to reduce frictional surface contact and keep the flow of lubricating water smooth to take away the hard particles and frictional heat. This section would focus on the material aspects including material modification and friction matching pairs optimization.

5.2.1 *Material modifications*

Wear-resistant modification is mainly based on fiber enhancement by using fiber materials with dimensional stability, high strength, high toughness, and environmental resistance to share the load on the contact surface. Besides, the presence of high-strength fibers could hinder the expansion of the fatigue cracks formed. Fiber materials used commonly are carbon fiber (CF), carbon nanofiber (CNF) or carbon nanotube (CNT), and glass fiber (GF). The wear-resistant modifications by fibers [79, 80, 165, 175, 176, 214–217] and solid particles [164, 168, 171, 172, 218] are shown in Fig. 13, and some blending modifications [164, 165, 168, 171, 172, 175, 176] can simultaneously achieve the purpose of improving the friction reduction and wear resistance of the material.

In addition, the orientation of the fibers in the polymer material also affects the wear resistance of the material, it would have a better effect when the fiber arrangement is perpendicular to the sliding direction [219]. To make the blended fiber orientation controllable, one or more fibers could be woven into a fabric with higher order, tightness, and integrity to improve the mechanical strength of the modified material which could bring better structural stability and higher loading capacity. Fabric reinforced technology

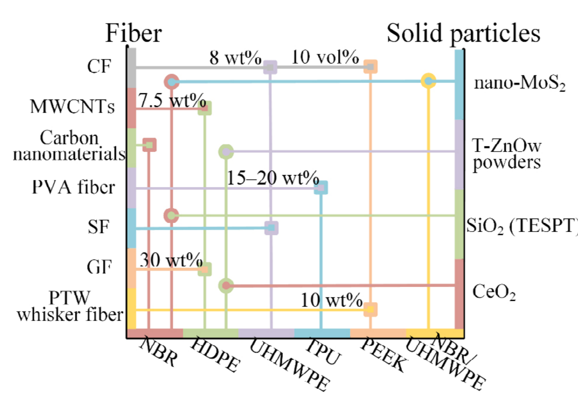

Fig. 13 Blending modification for wear resistance improvement.

has already been used in several commercial bearings [220]. Meanwhile, the water swelling of the filler should not be ignored, because it is easier for some hydrophilic or water-absorbing particles to fall off from the composite substrate in the wear process [168]. Falling materials would destroy the surface condition of the material and cause abrasive wear to increase the wear rate [221].

In some cases, the multi-composite modification of multiple fillers could take advantage of the synergistic effect between the components to obtain better tribological properties. This effect has been observed when CF is reinforced by nano-SiO_2 [222] or TiO_2 particles [223], CF and PTW synergistically reinforce PEEK [224], and 10 vol% Gr-10 vol% CF-5 vol% CNT modifies polyimide (PI) [225]. The components could share the load, and improve the interfacial combination between fillers and substrate to reduce stress concentration and achieve synergistic efficiency. However, it may also lead to increased wear, such as the addition of both CNT and SCF in PPS composites because the fillers cannot play a good interaction [226].

5.2.2 *Friction matching pairs optimization*

Abrasive wear in fluid lubrication depends on the hardness of the wear surface, the opposing surface, and the abrasive particles. It is effective for friction pairs to reduce the wear volume and improve the performance of abrasive wear resistance by decreasing the hardness of the abrasives or increasing the hardness of the wearing surface [227]. The research reviewed in Section 5.1.2 also indicates the same conclusion about improving the wear resistance of WLBs by increasing the hardness of the friction pairs. As shown in Table 8, some special surface treatments can be applied to improve the surface hardness.

However, Yuan et al. [238] showed that it was not enough to enhance the wear resistance only by increasing the surface hardness because the wear was affected by multiple factors (e.g., load, speed, lubrication water quality, etc.). Golchin et al. [239] supported that the deformation caused by plowing action could further lead to adhesive wear on the contact surface when the difference of the elastic modulus and surface free energy between the friction pairs was large. Quaglini et al. [240] concluded that polymers with low elastic modulus exhibited better sliding behavior on smooth interfaces, while polymers with high modulus could obtain better tribological properties when it was sliding on rough interfaces. The wear resistance improvement of bearings requires

Table 8 Surface treatment methods to improve the surface hardness of the friction pairs.

Surface treatment methods	Treated surfaces	Coatings	Effects	Ref.
Unbalanced magnetron sputtering (UBM)	The surface of Si_3N_4, SiC, and cemented carbide (WC)	Graphite-like carbon (GLC) films	Improved material hardness, loading capacity, self-lubrication effect, and reduced wear	[228]
	Si (100) wafers and 316L stainless steel substrates	Ti-DLC coatings	Reduced friction and wear	[229–231]
		TiN(C) coatings		
		CrSiBCN composite coatings		
	SiC surface	CrSiCN coatings		[232]
High-velocity oxyfuel spraying (HVOF)	Bearing steels	WC–Co coatings	60% increase in hardness	[233]
	WC and WB thermally sprayed coatings	Martensitic stainless steel	Increased surface hardness and reduced wear under water lubrication	[234]
Ni spraying coating	Ni thermally sprayed coatings			
Ion nitriding	Stainless steel	/	Improved surface hardness and wear resistance of stainless steel	[235]
	2Cr13 Steel	/	Better than quenched treatment	[236]
Proton irradiation	CF–PTFE	Defluoridation and carbonization of composite surfaces	Reduced surface wettability and surface energy, improved material wear resistance	[237]

an effective match of highly wear-resistant polymer bearings with surface hardened shafts [241]. The commonly used water-lubricated friction pairs are organized as shown in Table 9, which could provide guidance for engineering applications.

6 Generation mechanism and suppression methods of friction noise

Noise is generated by vibration. WLSBs are an important part of the marine propulsion system. It can be seen as a vibration component in shafting operation. Under special conditions (e.g., low speed, heavy load, or poor lubrication), it is easy to produce abnormal vibration and noise. Bharat Bhushan named the vibration noise at higher frequencies (560–1,670 Hz) as "Squeal" and lower frequencies (300–600 Hz) as "Chatter" in his research about WLRBs [249]. Besides, WLSBs can also be considered as a vibration isolation element in shafting system. It can weaken the excitation on the shaft (such as the excitation from the propeller or prime motor, etc.) to be transmitted outward to the bearing base or even the hull, and also reduce the external excitation (such as the excitation generated by waves on the hull, etc.) to be transmitted to the shaft.

The vibration-induced noise generated by these internal or external excitations would threat the stealthiness, reliability, and passenger comfort of the ship. The evolution mechanism of friction noise is required to improve the quiet level and survivability of ships. In this section, the evolution mechanism of the friction noise would be represented from the theoretical research and experiment test to propose the prevention methods from structure optimization and material modification.

6.1 Generation mechanism of friction noise

Theoretical research is mainly to establish the model to study the influencing factors or system coupling by reasonably simplifying the friction system; experimental research is to collect and analyze the signals (e.g., torque, displacement, vibration, etc.) to capture the vibration noise characteristics and analyze the generation mechanism.

6.1.1 Theoretical studies

The current research is mainly focused on automotive brakes, among which the relatively well-established and highly recognized explanatory mechanisms are shown in Table 10. The stick–slip mechanism and

Table 9 Commonly used water-lubricated friction pairs.

Matching type	Examples	Material hardness	Wear conditions	Applications	Ref.
Polymer and ceramic matching pairs	PEEK450-FC30/SiC	47HRC/≥90HRC	Adhesion and mechanical plowing	Seawater plunger pump	[242]
	CFPEEK/ Si_3N_4	19HRA/93HRA		/	[243]
	PEEK/ Si_3N_4	Shore D90/89HRC	Slight wear	Thrust bearing	[207]
	Polyurethane/ Si_3N_4	Shore D67/89HRC			
	PI/ Si_3N_4	122HV/1580HV	The dimples appeared on the surface	WLBs	[244]
Polymers and metal matching pairs	PEEK-CF30/2Cr13 Steel	47HRC/-	Corrosion in seawater	/	[209]
	PEEK / Aluminum bronze	Shore D96/ D 105	Adhesive and abrasive wear	Thrust bearing	[208]
	PEEK/ stainless steel	Shore D90/53HRC	/	Hydraulic turbine generator	[209]
	NBR/ 1Cr18Ni9Ti stainless steel	Shore A63/38HRA	Abrasive wear in sandy water	Ship stern tube bearings	[205]
	BGT rubber/ GCr15 steel	/	Abrasive wear	WLBs	[245]
Ceramic and metal matching pairs	Si_3N_4/316L	90HRA/-	Mechanical plowing	Ocean environment	[246]
Ceramic and ceramic matching pairs	Ti_3AlC_2/SiC	5.25GPa/≥90HRC	No obvious wear	Ocean environment	[247, 248]

Table 10 Mechanism of friction noise.

Theories	Ref.	Features
Stick-slip mechanism	[251]	Friction-induced vibrations exist in the intrinsic properties of the friction interface, especially the dependence of the friction coefficient on the sliding velocity.
Negative friction-velocity slope mechanism	[252]	
Sprag-slip mechanism	[253]	The geometry-induced or the kinematic-constrained instability caused by the system intrinsic structure contributes to the vibration and noise.
Modal coupling mechanism	[254, 255]	
Friction time-lag theory	[256, 257]	
Hammering theory	[258]	
Unified theory	[259, 260]	/

negative friction–velocity slope mechanism were used to explain the friction vibration and noise of WLBs. For example, the research on self-excited vibration of the shaft–bearing coupling system of Wu et al. [250] verified the negative friction–velocity slope mechanism.

Ibrahim believed that the factors considered in various mechanisms were not comprehensive enough. Therefore, the friction-induced phenomena (e.g., vibration, chatter, squeal, and chaos, etc.) because of the contact and frictional mechanics were systematically studied [261], which pointed out that the friction models of any dynamical system should be established according to the operating conditions and geometry of the system. The friction models adopted for different engineering applications were reviewed [262] and pointed out that it was necessary for WLBs to study the effect of friction on nonlinear modal coupling and explore the role of nonlinear coupling in the elimination of friction excitation. Simpson et al. [263] established a nonlinear dual-degree-of-freedom model for a submarine tailpipe bearing to analyze the nonlinear response of the coupling system and concluded that the bearing instability was mainly caused by the friction force varying nonlinearly with time and velocity.

In the real shaft system, the friction vibration of WLBs does not exist independently, which needs to pay attention to the coupling relationship between the non-linear friction excitation and the shaft system vibration generated by the bearing and the shaft or even the shaft system. Zhang et al. considered the torsional-lateral coupling through bearing-shaft interaction [264], and further investigated the effect of nonlinear friction on the propeller-shaft system [265]. The results showed that friction-induced system vibrations were caused by the coupling effects of interface nonlinear friction and system components [266]. The role of nonlinear coupling models in the study of friction vibration of WLBs is becoming more and more important [267]. Therefore, theoretical research must establish and solve the coupling models according to the actual influencing factors by considering the hydrodynamic effect, thermal effect, and the deformation effect of the bearing and shaft.

6.1.2 *Experimental studies*

Some experimental studies on frictional vibration noise are shown in Table 11. It shows that stick–slip and nonlinear frictional vibrations are considered as the main induced factors of vibration noise. In addition, Peng et al. [268] compared the spectrum characteristics of WLRBs when frictional vibration occurred and during normal operation, which provided a reference for the identification of abnormal friction noise in stern bearings. Dong et al. revealed the relationship between the lubrication properties of polymers and friction noise performance, which contributed to the material selection in bearing design [269].

Only through reasonable experimental design and visualization of friction vibration information can the characteristic information be captured, and the mechanism of friction vibration can be further revealed through experiments, which can provide verification and guidance for theoretical research and engineering application.

6.2 Suppression methods for friction noise

The vibration and noise problems of WLBs should be

Table 11 Experimental study of friction and vibration noise for WLBs.

Experiments	Contents	Results	Notes
A series of large disc tests [270–272]	Contact mechanics of bearing and dynamic characteristics of the relevant structural components	Relationship between structural damping and frictional vibration	Early experiments
Rubber and glass slider [249]		Squeal or chatter regimes depend on the load and sliding speed	
Vibration tests by Liu et al.	Friction vibration coupled with lateral vibration [91]	The interference of lateral vibration accelerated the instability of the system.	Numerical simulation and test
	The influence of the lateral vibration on the friction-induced vibration of WLSBs [273]	The normal vibration would aggravate the amplitude, and narrow the speed range of friction-induced vibration.	
	Water-lubricated rubber stern bearings [274]	Friction-induced vibration appeared at low speeds	/
	Water-lubricated rubber slat bearings [275]	Vibration spectrum characteristics explained by negative friction-velocity slope mechanism	/
	Nonlinear response of coupling vibration [276]	Conditions for noise generation and stick-slip occurrence	Nonlinear friction-induced vibrations due to negative damping at low speeds or viscous friction at high speeds
Reproduce the stick-slip nonlinear friction-induced vibrations [277]		Mechanism of stick-slip motion in shaft-bearing interface	
Visualization of frictional vibration information	Water-lubricated rubber stern bearings	Analyzed the mechanism of vibration noise generation [278]	Limitation of mate material selection, but a new idea for the study of friction and vibration noise evolution
		Revealed the coupling process of friction and torsional vibration in the stern system [279]	
	Rubber block with a brass shaft mating	Stick–slip was the root cause of friction vibration [280]	

solved by reducing bearing vibration and improving the vibration isolation capacity of bearing. The previous section indicates that the generation of friction noise is related to the self-excited vibration caused by the stick–slip motion and lubrication state change between friction pairs. The friction coefficient [281] and the ratio of static and dynamic friction coefficients [282] could also have an impact on friction noise. The prevention and control of friction noise need to be approached from both structure and material to improve the lubrication performance and reduce the friction coefficient fluctuations.

6.2.1 *Structure optimization*

Qin et al. pointed out that the significance of each factor on the effect of friction vibration was in the order of lubrication conditions, contact pressure, hardness, and rubber layer thickness. It is possible to reduce the friction vibration intensity of rubber bearings by increasing the rubber layer hardness, decreasing contact pressure or rubber layer thickness [280]. Jiang et al. [283] indicated that it was effective to control the abnormal vibration of rubber bearings by increasing the damping coefficient and Stribeck curve attenuation coefficient. Otherwise, the cooling water temperature [284] and the shape of the rubber slat surface [285] also could influence the friction vibration. The surface texture enabled the water-lubricated rubber slat bearings to reduce the critical speed and suppress the high-frequency friction vibration [275].

The above traditional structural optimization can play a certain vibration suppression effect. In addition, porous structure is one of the important means to improve the vibration and noise reduction performance of materials. Jin et al. designed a fluid-saturated perforated slab, which effectively reduced the vertical-direction vibration amplitude of WLSBs [286].

6.2.2 *Material modification*

It is possible for WLBs to suppress the friction noise by using the materials with better hydrophilicity, self-lubricating and viscoelasticity [269]. The self-excited vibration could be suppressed by large damping, high speed, and large support stiffness [250]. The elastic rubber pads with good damping performance could effectively reduce the vibration amplitude of thrust bearings [86].

The friction noise of bearings could also be reduced by improving the lubrication performance through material modification. Zhou et al. [167] modified NBR with a blending of UHMWPE and Gr powder to obtain a new composite rubber with a small negative slope of velocity change, which was not easy to occur stick–slip phenomena and suppressed the friction noise at low speed. The polymer material of WLSBs modified by GNS could improve the self-lubrication capability to reduce the friction vibration and noise during start/stop process [173]. The material modification could also improve the surface hardness and weaken the surface deformation to reduce the magnitude of the friction fluctuation. HDPE modified by MWCNTs [80] or tetrapod-like zinc oxide whisker (T-ZnOw) powder [171] could improve the hardness and compression strength to effectively reduce the friction coefficient and fluctuation.

6.2.3 *Damping-enhanced structure*

It is not sufficient to achieve the reduction goal of the frictional vibration and noise only by material modification, because the soft lining and rubber layer would deform and lose the damping effect under the heavy or bias load. The contradiction between high load capacity and high damping needs to be solved by carrying out the decoupling design, which requires adding an attachment structure to the bearing bushing or on the outer wall of the bearing to isolate vibration [287].

A damping-enhanced structure separating stiffness from damping can decouple the load carrying and damping functions. As shown in Fig. 14, the attachment structure must have a high stiffness k_2 to provide high load carrying capacity, and a large damping c_2 to achieve energy dissipation [287].

As shown in Fig. 15, the integral squeeze film damper (ISFD) technology is one of the effective methods for WLBs to achieve this damping-enhanced structure [287]. It is effective for the retained material S-type ISFD with the compact structure to solve the problem of nonlinear vibration and low critical speed

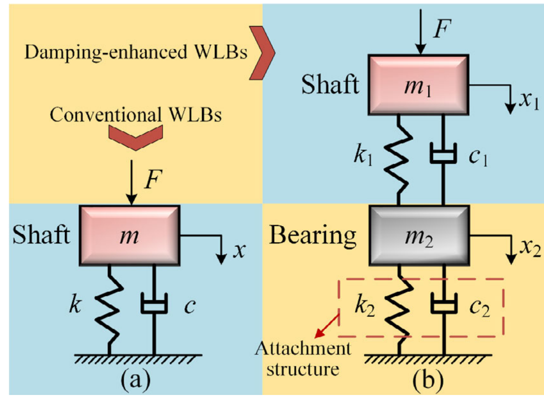

Fig. 14 Dynamic model: (a) conventional WLBs; (b) damping-enhanced WLBs. Reproduced with permission from Ref. [287], © The Brazilian Society of Mechanical Sciences and Engineering 2021.

of the rotor system [288]. The Wuhan University of Technology further proposed the application of magnetic fluid to SFD to achieve adjustable and controllable damping of the bearing [287, 289]; Mayank Tiwari et al. [290] made an ISFD filled with magnetorheological fluid and verified its vibration damping effect under different operating conditions through experiments.

In addition, metamaterials based on locally resonant sonic materials [291] have been applied in mechanical vibration control of rolling bearing box [292] and marine power equipment mount [293], and achieved good results. It is feasible to apply metamaterials to water-lubricated bearings. The reasonable design of metamaterials to make them suitable for water-lubricated bearings will be a breakthrough point to improve the bearing capacity and damping capacity of water-lubricated bearings.

In general, it is difficult for bearings to improve lubrication and reduce vibration only by traditional methods such as material modification and surface texture. It requires to combine with innovative structural designs such as damping-enhanced structure or magneto-hydraulic double floating to achieve the reduction of bearing vibration and noise.

7 Future study

Although the WLBs has seen a great deal of research in recent years some of the results have been applied on ships, but green and high-performance ships put forward new requirements for WLBs. There are still

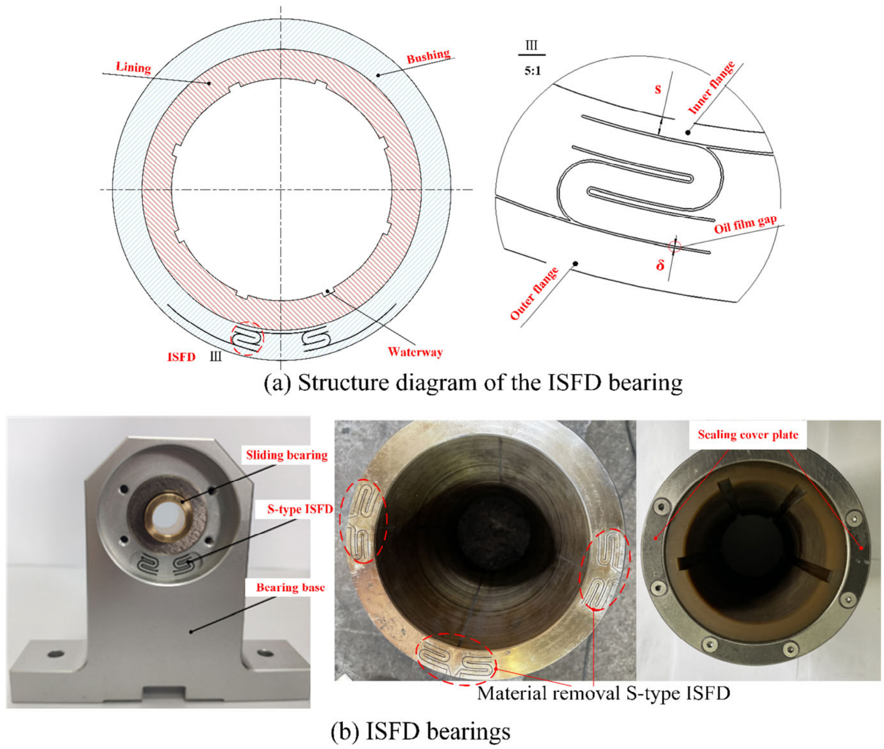

Fig. 15 ISFD structure and its application in bearings.

some urgent problems to be solved in theoretical research, test technology and intelligent operation and maintenance, etc.

7.1 Theory and mechanism research

To reflect the real lubrication state, the thermo-soft elastomeric transient mixed lubrication model should be developed by considering the thermal-fluid-solid coupling with material nonlinearity. The distributed mixed lubrication theory should be further developed by the identification of the lubrication state. Moreover, the complex interaction between lubrication, friction, wear, and vibration noise requires the following research to consider their evolution mechanism comprehensively, which would also become a theoretical basis for the research of intelligent operation and maintenance. In addition, it is necessary to establish the multi-constraint frictional vibration model of the bearing system. The shafting dynamics theory should be considered by analyzing partial contact states to describe the complex mechanism of vibration noise.

7.2 Develop more advanced test technology

New measurement technology for wear and load is an important development trend in the measurement of water-lubricated bearings. Combined with vibration monitoring, it will provide the possibility of intelligent bearings and shaft system. The single-point measurement should be replaced by distributed measurement with the application of sensor array testing technology to reflect the real lubrication state. In addition, the current test technologies are difficult to separate the friction vibration well, which requires deeper dynamic friction test methods with faster response rate and higher identification accuracy. Furthermore, it is necessary for WLBs to establish the mapping relationship between performance test and real ship operation to improve the mutual verification ability and residual life prediction.

7.3 Collaborative design of structure and material

At present, the material and structural design of WLBs is relatively independent. The collaborative design should be carried out by considering both material modification and structural optimization, especially when new materials are introduced into the WLBs. It should be taken load-carrying, friction, wear, and vibration noise as the overall optimization goal to develop prevention and control methods. Magneto-hydraulic double-suspension technology should be further developed to improve the performance stability and robustness of WLBs. The metamaterials technology and biomimetic technology combined with WLBs will be a beneficial attempt. Furthermore, the damping control of ISFD and other active control technologies, and embedded sensor technology will become an important trend in smart WLBs and shafting.

7.4 Establish standards and regulations

Compared with American standards with detailed provisions of the bearing (e.g., material performance indexes, test methods, and the test bench, methods, conditions, samples, indexes, etc.), the current standards in China only briefly regulate the structure and material of the integrated rubber bearings, which lacks of the standards of specific process planning procedure, performance testing methods, and index evaluations. Therefore, it is urgent to deal with the lack standards of WLSBs test and evaluation. In order to better ensure its service performance, a systematic and highly operational regulations should be established to enhance the system management.

7.5 Address the challenges of new-type ships

Due to the development of the electric direct-driven and integrated marine propulsion technology, the RDT would be more advantageous than the traditional shaft propulsion device because of its compact structure and higher efficiency. The water-lubricated thrust bearing with excellent performance is the key for RDT power to break through the megawatt-class. Moreover, the development of intelligent and less manned ships requires the establishment of intelligent operation and maintenance and health management of bearing/shafting in the whole life cycle to realize the intelligence of ship engine room.

8 Conclusions

With the trend of large-scale and high-speed development of ships, WLBs as a key component of ship propulsion shaft system play a more and more important role in the efficient, smooth, and safe operation of ships. The research of WLBs has distinct characteristics of demands, problems, and goals.

This paper summarized the lubrication principle and testing technology of WLBs, and focused on the mechanism and prevention methods of friction, wear, and noise of WLBs. While summarizing the performance improvement methods of WLBs with traditional structural optimization and material modification, the new methods for performance improvement were also reviewed.

(1) In the section of friction-reduction, the structure optimization technology of surface texture was mainly introduced, and the development and application of magneto-hydraulic double-suspension bearing technology were summarized. The main content of material modification was blending modification. In addition, the related research of bionic modification was introduced, and the potential application of ion implantation technology in WLBs was pointed out.

(2) According to different wear forms, the main wear mechanisms of WLBs were reviewed, and the influence of the two main factors of friction pairs hardness and operating conditions on bearing wear was summarized. Based on these, the material blending modification and friction matching pairs optimization technology were proposed to improve the wear resistance of bearing.

(3) The generation mechanisms of friction noise were reviewed and explained from two aspects of theoretical and experimental studies. In addition to the friction noise suppression methods of structural optimization and material modification, the related research of damping-enhanced structure was also summarized.

Extensive efforts have been carried out to improve the performance of WLBs, but there are still many bottlenecks to be overcome (e.g., the lubrication theory, wear and vibration mechanism, test technology, collaborative optimization ability, etc.). According to the research status of marine WLBs and the development trend of green and intelligent, the possible research directions in the future were proposed. With the continuous development and improvement of relevant research, WLBs can be reasonably expected to play a more critical role in ship propulsion systems in the future, and may have a profound influence on the green shipping industry as well.

Acknowledgements

This work was financially supported by the National Key R&D Program of China (No. 2018YFE0197600) and National Natural Science Foundation of China (No. 52071244).

Declaration of competing interest

The authors have no competing interests to declare that are relevant to the content of this article. The author Xinping YAN is the Editorial Board of Member of this journal.

References

[1] Zhang S W. Green tribology: Fundamentals and future development. *Friction* **1**(2): 186–194 (2013)

[2] Yan X, Liang X, Liu Z, Zhou X, Yuan C, Ouyang W. Research progress of marine water lubricated stern bearing. *Ship Building of China* **58**(3): 221–232 (2017)

[3] Dong C L, Bai X Q, Yan X P, Yuan C Q. Research status and advances on tribological study of materials under ocean environment. *Tribology* **33**(3): 311–320 (2013) (in Chinese)

[4] Sommerfeld A. Zur hydrodynamischen theorie der schmiermittelreibung (on the hydrodynamic theory of lubrication). *Zeit Math Phys Bd* **50**: 97–155 (1904)

[5] DuBois G B, Ocvirk F W. Analytical derivation and experimental evaluation of short-bearing approximation for full journal bearings. *Natl Advis Comm Aeronaut NACA Repor* 1199–1230 (1953)

[6] Majumdar B C, Pai R, Hargreaves D J. Analysis of water-lubricated journal bearings with multiple axial grooves. *Proc Inst Mech Eng Part J J Eng Tribol* **218**(2): 135–146 (2004)

[7] Dousti S, Cao J M, Younan A, Allaire P, Dimond T. Temporal and convective inertia effects in plain journal bearings with eccentricity, velocity and acceleration. *J Tribol* **134**(3): 505–512 (2012)

[8] Dousti S, Fittro R L. An extended reynolds equation including the lubricant inertia effects: application to finite length water lubricated bearings. In *ASME Turbo Expo 2015: Turbine Technical Conference and Exposition*, Montreal, Quebec, Canada, 2015.

[9] Wang X F, Lin Q, Hu M H, Tang Y M, Hai P Z. A research on the mechanism of water-lubricated rubber stern-tube bearing. *Ship Eng* **15**(04): 45–49 (1993) (in Chinese)

[10] Litwin W. Influence of local bush wear on water lubricated sliding bearing load carrying capacity. *Tribol Int* **103**: 352–358 (2016)

[11] Shi F H, Salant R F. A mixed soft elastohydrodynamic lubrication model with interasperity cavitation and surface shear deformation. *J Tribol* **122**(1): 308–316 (2000)

[12] Hooke C J, O'Donoghue J P. Elastohydrodynamic lubrication of soft, highly deformed contacts. *J Mech Eng Sci* **14**(1): 34–48 (1972)

[13] Huang P, Zheng J, Hooke C, Wen S Z. Effect of roughness on lubrication of low elastic modulus in line contact. *Journal of Tsinghua University (Science and Technology)* **36**(10): 50–55 (1996) (in Chinese)

[14] Hooke C J. Roughness in soft elastohydrodynamically lubricated contacts–Attenuation and the complementary wave reassessed. *Proc Inst Mech Eng Part J J Eng Tribol* **230**(11): 1325–1335 (2016)

[15] Wilcock D F, Booser E R. *Bearing Design and Application*. McGraw-Hill, 1957.

[16] Dowson D. A generalized Reynolds equation for fluid-film lubrication. *Int J Mech Sci* **4**(2): 159–170 (1962)

[17] Li Z, Wang F C, Yuan X Y, Zhu J. Analysis of thermodynamic lubrication performance of helical surface sectoral tile thrust bearing. *Mechanical Science and Technology* **18**(3): 69–71 (1999) (in Chinese)

[18] Glavatskih S B, Fillon M. TEHD analysis of thrust bearings with PTFE-faced pads. *J Tribol* **128**(1): 49–58 (2006)

[19] Wodtke M, Fillon M, Schubert A, Wasilczuk M. Study of the influence of heat convection coefficient on predicted performance of a large tilting-pad thrust bearing. *J Tribol* **135**(2): 21701–21702 (2013)

[20] Wodtke M, Schubert A, Fillon M, Wasilczuk M, Pajączkowski P. Large hydrodynamic thrust bearing: Comparison of the calculations and measurements. *Proc Inst Mech Eng Part J J Eng Tribol* **228**(9): 974–983 (2014)

[21] Zhai L M, Luo Y Y, Liu X, Chen F N, Xiao Y X, Wang Z W. Numerical simulations for the fluid-thermal-structural interaction lubrication in a tilting pad thrust bearing. *Eng Comput* **34**(4): 1149–1165 (2017)

[22] Wodtke M, Olszewski A, Wasilczuk M. Application of the fluid–structure interaction technique for the analysis of hydrodynamic lubrication problems. *Proc Inst Mech Eng Part J J Eng Tribol* **227**(8): 888–897 (2013)

[23] Tzeng S T, Saibel E. Surface roughness effect on slider bearing lubrication. *S L E Trans* **10**(3): 334–348 (1967)

[24] Christensen H, Tonder K. The hydrodynamic lubrication of rough bearing surfaces of finite width. *J Lubr Technol* **93**(3): 324–329 (1971)

[25] Christensen H, Tonder K. The hydrodynamic lubrication of rough journal bearings. *J Lubr Technol* **95**(2): 166–172 (1973)

[26] Patir N. A numerical procedure for random generation of rough surfaces. *Wear* **47**(2): 263–277 (1978)

[27] Patir N, Cheng H S. Application of average flow model to lubrication between rough sliding surfaces. *J Lubr Technol* **101**(2): 220–229 (1979)

[28] Patir N, Cheng H S. An average flow model for determining effects of three-dimensional roughness on partial hydrodynamic lubrication. *J Lubr Technol* **100**(1): 12–17 (1978)

[29] Wu C W, Zheng L Q. An average Reynolds equation for partial film lubrication with a contact factor. *J Tribol* **111**(1): 188–191 (1989)

[30] Greenwood J A, Tripp J H. The contact of two nominally flat rough surfaces. *Proc Inst Mech Eng* **185**(1): 625–633 (1970)

[31] de Kraker A, van Ostayen R A J, Rixen D J. Calculation of Stribeck curves for (water) lubricated journal bearings. *Tribol Int* **40**(3): 459–469 (2007)

[32] Zhang H, Hua M, Dong G N, Zhang D Y, Chin K S. A mixed lubrication model for studying tribological behaviors of surface texturing. *Tribol Int* **93**: 583–592 (2016)

[33] Venner C H, ten Napel W E. Surface roughness effects in an EHL line contact. *J Tribol* **114**(3): 616–622 (1992)

[34] Venner C H, Lubrecht A A. Transient analysis of surface features in an EHL line contact in the case of sliding. *J Tribol* **116**(2): 186–193 (1994)

[35] Geike T, Popov V. Cavitation within the framework of reduced description of mixed lubrication. *Tribol Int* **42**(1): 93–98 (2009)

[36] Gohar R, Cameron A. Optical measurement of oil film thickness under elasto-hydrodynamic lubrication. *Nature* **200**(4905): 458–459 (1963)

[37] Spikes H A, Cann P M. The development and application of the spacer layer imaging method for measuring lubricant film thickness. *Proc Inst Mech Eng Part J J Eng Tribol* **215**(3): 261–277 (2001)

[38] Hartl M, Krupka I, Poliscuk R, Liska M, Molimard J, Querry M, Vergne P. Thin film colorimetric interferometry. *Tribol Trans* **44**(2): 270–276 (2001)

[39] Jiang X F, Hua D Y, Cheng H S, Ai X L, Lee S C. A mixed elastohydrodynamic lubrication model with asperity contact. *J Tribol* **121**(3): 481–491 (1999)

[40] Han Y F, Xiong S W, Wang J X, Jane Wang Q. A new singularity treatment approach for journal-bearing mixed lubrication modeled by the finite difference method with a herringbone mesh. *J Tribol* **138**(1): 11704 (2016)

[41] Ouyang W, Chen R L, Peng L, et al. Main stiffness and main damping of sliding bearings considering local contact. *Journal of Xi'an Jiaotong University* **48**(1): 112–117 (2014) (in Chinese)

[42] Li J, Ouyang W, Liu Q, Zhang Z, Zhang Y. Film-thickness identification method and lubrication characteristic experiment of full-size water-lubricated stern bearing under offset load. *Sensors* (*Basel*) **22**(10): 3670 (2022)

[43] Ettles C M M. The analysis and performance of pivoted pad journal bearings considering thermal and elastic effects. *J Lubr Technol* **102**(2): 182–191 (1980)

[44] Hashimoto H, Wada S. Turbulent lubrication of tilting-pad thrust bearings with thermal and elastic deformations. *J Tribol* **107**(1): 82–86 (1985)

[45] Liang X X, Yan X P, Ouyang W, Wood R J K, Liu Z L. Thermo-Elasto-Hydrodynamic analysis and optimization of rubber-supported water-lubricated thrust bearings with polymer coated pads. *Tribol Int* **138**: 365–379 (2019)

[46] Sternlicht B, Carter G K, Arwas E B. Adiabatic analysis of elastic, centrally pivoted, sector, thrust-bearing pads. *J Appl Mech* **28**(2): 179–187 (1961)

[47] Hu Y Z, Zhu D. A full numerical solution to the mixed lubrication in point contacts. *J Tribol* **122**(1): 1–9 (2000)

[48] Liu S B, Wang Q, Liu G. A versatile method of discrete convolution and FFT (DC-FFT) for contact analyses. *Wear* **243**(1–2): 101–111 (2000)

[49] Liu S B, Wang Q. Studying contact stress fields caused by surface tractions with a discrete convolution and fast Fourier transform algorithm. *J Tribol* **124**(1): 36–45 (2002)

[50] Di Benedetto G, Organisciak M, Popovici G. Film thickness prediction of radial lip seal. *FME Transactions* **37**(2): 211–214 (2009)

[51] Li S, Kahraman A. A mixed EHL model with asymmetric integrated control volume discretization. *Tribol Int* **42**(8): 1163–1172 (2009)

[52] Ahmed S, Goodyer C E, Jimack P K. An adaptive finite element procedure for fully-coupled point contact elastohydrodynamic lubrication problems. *Comput Methods Appl Mech Eng* **282**: 1–21 (2014)

[53] Wang Y C, Liu Y, Huang W F, Guo F, Wang Y M. The progress and engineering application of theoretical model for mixed lubrication. *Tribology* **36**(04): 520–530 (2016)

[54] Zhao Z M, Zhang R. Theoretical and experimental analysis of a water-lubricated rubber journal bearing with a large aspect ratio. *Ind Lubr Tribol* **72**(6): 797–803 (2020)

[55] Hu Q, Hu J, Ye X, Zhang D, Zheng J. Flow field distribution of liquid film of water lubricated bearing-rotor coupling systems. In *7TH International Conference on Pumps And Fans (ICPF2015)*, 2016: 12056.

[56] Zhou G, Li P, Liao D, Zhang Y, Zhong P. The friction-induced vibration of water-lubricated rubber bearings during the shutdown process. *Materials* (*Basel*) **13**(24): E5818 (2020)

[57] Liao Y F, Zhou Y. Analysis on the lubrication characteristics of a few aqueous media that affect water lubricated rubber alloy bearing. *J Mech Sci Technol* **31**(10): 4771–4779 (2017)

[58] Wang Y Z, Li L H, Zhong T, Yin W Z. Simulation and experimental study on lubrication performances of uhmwpe-based water lubricated stern bearing. *Lubr Eng* **46**(02): 17–23 (2021)

[59] Liu Y, Lao X S, Dai C H, Yao S W. Numerical simulation analysis of fluid-solid coupling of water-iubricated bearings. *IOP Conf Ser Mater Sci Eng* **1133**(1): 12003 (2021)

[60] Zhang H, Yuan C Q, Tan Z S. A novel approach to investigate temperature field evolution of water lubricated stern bearings (WLSBs) under hydrodynamic lubrication. *Adv Mech Eng* **13**(2): 168781402199296 (2021)

[61] Ouyang W, Cheng Q C, Jin Y, Liu Q L, Wang B, Wang L. Lubrication performance distribution of large aspect ratio water-lubricated bearings considering deformation and shaft bending. *Tribol Trans* **64**(4): 730–743 (2021)

[62] Han Y F, Tang T, Xiang G, Jia H. A fluid–solid–heat coupling analysis for water-lubricated rubber stern bearing considering the deflection of propeller shaft. *Appl Sci* **11**(3): 1170 (2021)

[63] Xiang G, Han Y F, He T, Wang J X, Xiao K. A dynamic wear model for micro-grooved water-lubricated bearings under transient mixed lubrication condition. *J Tribol* **142**(7): 071701 (2020)

[64] Wang J F, Han Y F, Geng Z B, Xiang G, Wang J X, Zhao R. A profile design method to improve the wear performance of misaligned water-lubricated bearing. *Lubr Sci* **33**(5): 215–228 (2021)

[65] Jin D, Xiao K, Xiang G, Wang Y J, Wang C, Jia H. A simulation model to comparative analysis the effect of texture bottom shape on wear and lubrication performances for micro-groove water lubricated bearings. *Surf Topogr Metrol Prop* **9**(2): 025009 (2021)

[66] Xiang G, Yang T Y, Ning Q, Zhou C D, Wang C, Lv Z L. Numerical study on transient mixed lubrication response for multiple grooves water-lubricated bearings under non-linear shock with 3D thermal effect. *Surf Topogr Metrol Prop* **9**(3): 035014 (2021)

[67] Feng W, Han Y F, Xiang G, Wang J X. Hydrodynamic lubrication analysis of water-lubricated bearings with partial microgroove considering wall slip. *Surf Topogr Metrol Prop* **9**(1): 015019 (2021)

[68] Xiang G, Han Y F, Chen R X, Wang J X, Ni X K, Xiao K. A hydrodynamic lubrication model and comparative analysis for coupled microgroove journal-thrust bearings lubricated with water. *Proc Inst Mech Eng Part J J Eng Tribol* **234**(11): 1755–1770 (2020)

[69] Xiang G, Han Y F, Wang J X, Xiao K, Li J Y. Influence of axial microvibration on the transient hydrodynamic lubrication performance of misaligned journal-thrust microgrooved coupled bearings under water lubrication. *Tribol Trans* **64**(4): 579–592 (2021)

[70] Yang J, Palazzolo A. Three-dimensional thermo-elasto-hydrodynamic computational fluid dynamics model of a tilting pad journal bearing—Part I: Static response. *J Tribol* **141**(6): 061702 (2019)

[71] Yang J, Palazzolo A. Three-dimensional thermo-elasto-hydrodynamic computational fluid dynamics model of a tilting pad journal bearing—Part II: Dynamic response. *J Tribol* **141**(6): 061703 (2019)

[72] Yang J, Palazzolo A. Computational fluid dynamics based mixing prediction for tilt pad journal bearing TEHD modeling—Part I: TEHD-CFD model validation and improvements. *J Tribol* **143**(1): 011801 (2021)

[73] Yang J, Palazzolo A. Computational fluid dynamics based mixing prediction for tilt pad journal bearing TEHD modeling—Part II: Implementation with machine learning. *J Tribol* **143**(1): 011802 (2021)

[74] Liang X X, Yan X P, Liu Z L, Ouyang W. Effect of perturbation amplitudes on water film stiffness coefficients of water-lubricated plain journal bearings based on CFD–FSI methods. *Proc Inst Mech Eng Part J J Eng Tribol* **233**(7): 1003–1015 (2019)

[75] Sun F X, Zhang X B, Wei Y S, Wang X, Wang D. Stability analysis of rubber-supported thrust bearing in a rotor-bearing system used in marine thrusters under disturbing moments. *Tribol Int* **151**: 106356 (2020)

[76] Jiang S Y, Liu P F, Lin X H. Study on static characteristics of water-lubricated textured spiral groove thrust bearing using laminar cavitating flow lubrication model. *J Tribol* **144**(4): 041803 (2022)

[77] Feng H H, Peng L P. Numerical analysis of water-lubricated thrust bearing with groove texture considering turbulence and cavitation. *Ind Lubr Tribol* **70**(6): 1127–1136 (2018)

[78] Orndorff R L JR. Water-lubricated rubber bearings, history and new developments. *Nav Eng J* **97**(7): 39–52 (1985)

[79] Hu D, Guo Z W, Jun T, Yuan C Q. A novel hydrophilic PVA fiber reinforced thermoplastic polyurethane materials for water-lubricated stern bearing. *Fibers Polym* **22**(1): 171–183 (2021)

[80] Wu Y H, Dong C L, Yuan C Q, Bai X Q, Zhang L Y, Tian Y. MWCNTs filled high-density polyethylene composites to improve tribological performance. *Wear* **477**: 203776 (2021)

[81] Dong C L, Yuan C Q, Xu A J, Bai X Q, Tian Y. Rippled polymer surface generated by stick–slip friction. *Langmuir* **35**(7): 2878–2884 (2019)

[82] Liu Q L, Ouyang W, Cheng Q C, Li J J, Cheng Q Z, Li R Q. Influences of bidirectional shaft inclination on lubrication and dynamic characteristics of the water-lubricated stern bearing. *Mech Syst Signal Process* **169**: 108623 (2022)

[83] Ouyang W, Liu Q L, Cheng Q C, Wan G, Jin Y. Identification of distributed dynamic characteristics of journal bearing with large aspect ratio under shaft bending. *J Mar Sci Eng* **10**(5): 658 (2022)

[84] Ning C X, Yan X P, Ouyang W. Load-sharing characteristics of water-lubricated rubber elastic supported tilting-pad thrust bearing for rim-driven thrusters. *J Traffic Transport Eng* **21**(02): 138–149 (2021) (in Chinese)

[85] Jin Y, Zheng L L. Research on fault diagnosis of ship stern bearing based on vibration analysis. *Adv Mater Res* **139–141**: 2354–2358 (2010)

[86] Liang X X, Yan X P, Wu O Y, Liu Z L. Experimental research on tribological and vibration performance of water-lubricated hydrodynamic thrust bearings used in marine shaft-less rim driven thrusters. *Wear* **426–427**: 778–791 (2019)

[87] Liang X X, Yan X P, Ouyang W, Wood R J K, Kuang F M, Liu Z L, Zhou X C. Comparison of measured and calculated water film thickness of a water-lubricated elastically supported tilting pad thrust bearing. *Surf Topogr Metrol Prop* **7**(4): 045010 (2019)

[88] Zhang C, Xie D C, Huang Q W, Wang Z H. Experimental research on the vibration of ship propulsion shaft under hull deformation excitations on bearings. *Shock Vib* **2019**: 1–15 (2019)

[89] Zhang C, Huang Q, Experimental research on the characteristics of ship propulsion system under dynamic excitations. In *2017 4th International Conference on Transportation Information and Safety (ICTIS)*, IEEE, 2017: 204–210.

[90] Huang Q W, Yan X P, Zhang C, Zhu H H. Coupled transverse and torsional vibrations of the marine propeller shaft with multiple impact factors. *Ocean Eng* **178**: 48–58 (2019)

[91] Jin Y, Liu Z L, Zhou X C. Theoretical, numerical, and experimental studies on friction vibration of marine water-lubricated bearing coupled with lateral vibration. *J Mar Sci Technol* **25**(1): 298–311 (2020)

[92] Litwin W. Experimental research on water lubricated three layer sliding bearing with lubrication grooves in the upper part of the bush and its comparison with a rubber bearing. *Tribol Int* **82**: 153–161 (2015)

[93] Liu G, Li M. Experimental study on the lubrication characteristics of water-lubricated rubber bearings at high rotating speeds. *Tribol Int* **157**: 106868 (2021)

[94] Wang N, Meng Q F. Research on wireless nondestructive monitoring method for film pressure of water-lubricated bearing. *Ind Lubr Tribol* **67**(4): 349–358 (2015)

[95] Li P J, Zhu Y S, Yan K, Xiong Q Q, Zhang Y Y. Experimental investigation on the film pressure measurement in microgap water-lubricated hybrid journal bearing. *Tribol Trans* **60**(5): 814–823 (2017)

[96] Ko P L, Chuang K C, Ma C C. A fiber Bragg grating-based thin-film sensor for measuring dynamic water pressure. *IEEE Sens J* **18**(18): 7383–7391 (2018)

[97] Valkonen A, Juhanko J, Kuosmanen P. Measurement of oil film pressure in hydrodynamic journal bearings. In *7th International DAAAM baltic Conference" Industrial Engineering"*, Tallin, Estonia, 2010: 1–6.

[98] Cui K, Hong Y P, Sui D D, Liu W Y, Zhang H X. A lossless fiber pressure sensor based on PDMS. *IEEE Access* **8**: 189036–189042

[99] Cabrera D L, Woolley N H, Allanson D R, Tridimas Y D. Film pressure distribution in water-lubricated rubber journal bearings. *Proc Inst Mech Eng Part J J Eng Tribol* **219**(2): 125–132 (2005)

[100] Rajala S, Lekkala J. PVDF and EMFi sensor materials—A comparative study. *Procedia Eng* **5**: 862–865 (2010)

[101] Karki S, Lekkala J. Film-type transducer materials PVDF and EMFi in the measurement of heart and respiration

rates. In *2008 30th Annual International Conference of the IEEE Engineering in Medicine and Biology Society*, Vancouver, BC, Canada, IEEE, 2008: 530–533.

[102] Rajala S, Lekkala J. Film-type sensor materials PVDF and EMFi in measurement of cardiorespiratory signals—A review. *IEEE Sens J* **12**(3): 439–446 (2012)

[103] Kärki S, Lekkala J. A new method to measure heart rate with EMFi and PVDF materials. *J Med Eng Technol* **33**(7): 551–558 (2009)

[104] Chen C M, Jing J P, Cong J Q, Ji C. Experimentally study of dynamic pressure distribution and oil film forces in journal bearing using ElectroMechanical Film sensor array. *Proc Inst Mech Eng C J Mech Eng Sci* **234**(4): 903–913 (2020)

[105] Xie Z L, Shen N W, Zhu W D, Tian W C, Hao L. Theoretical and experimental investigation on the influences of misalignment on the lubrication performances and lubrication regimes transition of water lubricated bearing. *Mech Syst Signal Process* **149**: 107211 (2021)

[106] Magdun O, Gemeinder Y, Binder A. Investigation of influence of bearing load and bearing temperature on EDM bearing currents. *In 2010 IEEE Energy Conversion Congress and Exposition*, Atlanta, GA, USA, 2010: 2733–2738

[107] Wang X F, Guo Y X, Xiong L. Hybrid fiber Bragg grating sensor for vibration and temperature monitoring of a train bearing. *Chin Opt Lett* **16**(7): 070604 (2018)

[108] Dong Y F, Zhou Z D, Liu Z C, Zheng K. Temperature field measurement of spindle ball bearing under radial force based on fiber Bragg grating sensors. *Adv Mech Eng* **7**(12): 168781401562033 (2015)

[109] Bhardwaj V, Pandey R K, Agarwal V K. Performance studies of textured race ball bearing. *Ind Lubr Tribol* **71**(9): 1116–1123 (2019)

[110] Yan K, Yan B, Li B Q, Hong J. Investigation of bearing inner ring-cage thermal characteristics based on CdTe quantum dots fluorescence thermometry. *Appl Therm Eng* **114**: 279–286 (2017)

[111] Lagowski J, Savtchouk A, Wilson M D. Steady state method for measuring the thickness and the capacitance of ultra thin dielectric in the presence of substantial leakage current. US2002130674(A1), 2002-9-19.

[112] Henry Y, Bouyer J, Fillon M. An experimental hydrodynamic thrust bearing device and its application to the study of a tapered-land thrust bearing. *J Tribol* **136**(2): 021703 (2014)

[113] Zhang F, Ouyang W, Xi Y H, Yuan X Y. Study on the lubrication performance and take-off speed of the nuclear main pump water lubricated bearing. *Mach Des & Res* **33**(5): 87–92 (2017) (in Chinese)

[114] Guo A N, Wang X J, Jin J, Hua D Y, Hua Z K. Experimental test of static and dynamic characteristics of tilting-pad thrust bearings. *Adv Mech Eng* **7**(7): 168781401559387 (2015)

[115] Poll G, Gabelli A. Formation of lubricant film in rotary sealing contacts: Part II—A new measuring principle for lubricant film thickness. *J Tribol* **114**(2): 290–296 (1992)

[116] Myant C, Reddyhoff T, Spikes H A. Laser-induced fluorescence for film thickness mapping in pure sliding lubricated, compliant, contacts. *Tribol Int* **43**(11): 1960–1969 (2010)

[117] Fowell M T, Myant C, Spikes H A, Kadiric A. A study of lubricant film thickness in compliant contacts of elastomeric seal materials using a laser induced fluorescence technique. *Tribol Int* **80**: 76–89 (2014)

[118] Ponjavic A, Chennaoui M, Wong J S S. Through-thickness velocity profile measurements in an elastohydrodynamic contact. *Tribol Lett* **50**(2): 261–277 (2013)

[119] Myant C, Fowell M, Spikes H A, Stokes J R. An investigation of lubricant film thickness in sliding compliant contacts. *Tribol Trans* **53**(5): 684–694 (2010)

[120] Huang P, Luo J B, Zou Q, Wen S Z. Ngy-2,interferometer for nanometer lubrication film thickness measurement. *Tribology* **14**(2): 175-179 (1994) (in Chinese)

[121] Richards S C, Roberts A D. Boundary lubrication of rubber by aqueous surfactant. *J Phys D*: *Appl Phys* **25**(1A): A76–A80 (1992)

[122] Sun, X G, Dai, J M, Cong, D C, Chu, Z X. Development of oil film thickness measuring system for thrust bearing. *Acta Metrol Sin* (2): 92–94 (2003) (in Chinese)

[123] Zhang X D, Guo Q, Niu H. Optical fiber measurement system for thickness of water film. *Opt Precis Eng* **23**(10): 2747–2754 (2015)

[124] Zhou G. Mixed lubrication analysis and dynamic performance optimization of water lubricated rubber alloy bearings. Ph.D. Thesis. Chongqing (China): Chongqing University, 2013.

[125] Bongaerts J H H, Day J P R, Marriott C, Pudney P D A, Williamson A M. *In situ* confocal Raman spectroscopy of lubricants in a soft elastohydrodynamic tribological contact. *J Appl Phys* **104**(1): 014913 (2008)

[126] Jiang, G D, Xie, Y B. The time domain multi-conditions identifying method of oil film coefficients of journal bearings. *Mech Sci Technol* **19**(1): 123–124, 136 (2000) (in Chinese)

[127] Zheng T S, Xu Q Y. Identifecati0n of journal bearing 0il-film dynamic coefficients by attaching additional masses to a rotor. *J Xi'an Jiaotong Univ* **26**(3): 99–106 (1992) (in Chinese)

[128] Ma J K, Liu Y F, Lu C H, Zhang L C. Study on identification of dynamic characteristics of oil-bearings based on unbalance response. *J Shandong Univ Technol* **31**(1): 38–42 (2001) (in Chinese)

[129] Yan K J, Duan J, Liu J, Zhou Y. A study on the field identification of large journal bearing oil film dynamic property coefficient. *J Xi'an Univ Technol* **13**(1): 64–68 (1997) (in Chinese)

[130] Du Y Y, Li M, Liu G, Li Z G, Hou G Q. Lubrication characteristics of water-lubricated rubber bearings in mixed-flow lubrication. *Journal of Xi'an Jiaotong University* **54**(9): 49–57 (2020) (in Chinese)

[131] Wang L, Wang X Y, Jiang X P, Wang X W, Wu G Q, Ye X Y, Ning J N. Dynamic and static characteristics of water lubricated tilting pad bearings. *J Drain Irrigat Mach Eng* **38**(2): 163–169 (2020) (in Chinese)

[132] Litwin W, Dymarski C. Experimental research on water-lubricated marine stern tube bearings in conditions of improper lubrication and cooling causing rapid bush wear. *Tribol Int* **95**: 449–455 (2016)

[133] Litwin W. Properties comparison of rubber and three layer PTFE-NBR-bronze water lubricated bearings with lubricating grooves along entire bush circumference based on experimental tests. *Tribol Int* **90**: 404–411 (2015)

[134] Wang L, Pei S Y, Xiong X Z, Xu H. Study on the static performance and stability of a water-lubricated hybrid bearing with circumferential grooves and stepped recesses considering the influence of recess sizes. *Tribol Trans* **57**(1): 36–45 (2014)

[135] Wang S, Ouyang W, Jin Y, Wang L, Deng T. Analysis of static characteristics of wave bearings considering elastic deformation. *J Ship Mech* **24**(11): 1443–1452 (2020)

[136] Wu S. Lubrication performance and thermal structure coupled analysis of water lubricated rubber alloy slab bearings. Master Thesis. Chongqing: Chongqing University, 2011.

[137] Zhang H, Tan Z S, Yuan C Q. Research progress of structure design for water lubricated stern bearings. *Lubrication Engineering* **45**(08): 120–129 (2020) (in Chinese)

[138] Zhang X L, Yin Z W, Jiang D, Gao G Y, Wang Y Z, Wang X B. Load carrying capacity of misaligned hydrodynamic water-lubricated plain journal bearings with rigid bush materials. *Tribol Int* **99**: 1–13 (2016)

[139] Liang X X, Liu Z L, Wang H J, Zhou X H, Zhou X C. Hydrodynamic lubrication of partial textured sliding journal bearing based on three-dimensional CFD. *Ind Lubr Tribol* **68**(1): 106–115 (2016)

[140] Gong J Y, Jin Y, Liu Z L, Jiang H, Xiao M H. Study on influencing factors of lubrication performance of water-lubricated micro-groove bearing. *Tribol Int* **129**: 390–397 (2019)

[141] Wang H J, Liu Z L. The influence of surface texture on tribological characteristics of water-lubricated rubber bearing. *J Phys*: *Conf Ser* **2029**(1): 012083 (2021)

[142] Guo Z W, Xie X, Yuan C Q, Bai X Q. Study on influence of micro convex textures on tribological performances of UHMWPE material under the water-lubricated conditions. *Wear* **426–427**: 1327–1335 (2019)

[143] Chang T, Guo Z W, Yuan C Q. Study on influence of Koch snowflake surface texture on tribological performance for marine water-lubricated bearings. *Tribol Int* **129**: 29–37 (2019)

[144] Hu D, Guo Z W, Xie X, Yuan C Q. Effect of spherical-convex surface texture on tribological performance of water-lubricated bearing. *Tribol Int* **134**: 341–351 (2019)

[145] Cui Z T, Guo Z W, Yuan C Q. Influence of different rhombic surface textures on the tribological performance of water-lubricated bearings. *Mat Express* **10**(9): 1452–1462 (2020)

[146] Guo Z W, Huang Q R, Xie X, Yuan C Q. Effects of spherical-platform texture parameters on the tribological performance of water-lubricated bearings. *Wear* **477**: 203863 (2021)

[147] Pei S, Xu H, Ma S, Di X. Multiscale method for modeling surface texture effects in hydrodynamic lubrication regime. *Journal of Xi'an Jiaotong University* **45**(5): 119–126 (2011)

[148] Li C, Pei S, Zheng W, Jiang R, Xu H, Hong J. Effects of surface texture on static and dynamic performances of offset bearings. *Lubrication Engineering* **5**(45): 18–24 (2020) (in Chinese)

[149] Geng Y, Chen W. Multiscale method of modelling surface texture with mass-conserving cavitation model. *Tribol Int* **173**: 107663 (2022)

[150] Kataoka H, Kimura Y, Fujita H, Takatani S. Measurement of the rotor motion and corresponding hemolysis of a centrifugal blood pump with a magnetic and hydrodynamic hybrid bearing. *Artif Organs* **29**(7): 547–556 (2005)

[151] Tan Q C, Li W, Liu B. Investigations on a permanent magnetic-hydrodynamic hybrid journal bearing. *Tribol Int* **35**(7): 443–448 (2002)

[152] Samanta P, Hirani H. Magnetic bearing configurations: Theoretical and experimental studies. *IEEE Trans Magn* **44**(2): 292–300 (2008)

[153] Muzakkir S M, Hirani H. Maintenance free bearings. *Int J Eng Res* **4**(3): 133–136 (2015)

[154] Chen R, Xu J, Wei Y, Yuan X. Static and dynamic characteristics of superconducting magnetic force and

hydrostatic fluid film force compound bearings. *Tribology* **36**(05): 531–537 (2016)

[155] Xu J M, Li C H, Miao X S, Zhang C P, Yuan X Y. An overview of bearing candidates for the next generation of reusable liquid rocket turbopumps. *Chin J Mech Eng* **33**: 26 (2020)

[156] Zhao, J H, Wang, Q, Zhang, B, Chen, T, Gao, D R. Research on static bearing characteristics of magnetic-liquid double suspension bearing. *High Technol Lett* **25**(4): 434–442 (2019)

[157] Wang S T, Wu O Y, Li Z, Wang B. Load carrying capacity of a novel magnetic-liquid double suspension fixed pad thrust bearing. *Ind Lubr Tribol* **73**(2): 381–387 (2021)

[158] Ouyang W, Li Z, Wang S T. A kind of bullet-supported tiltable tile magneto-hydraulic double-floating thrust bearing. CN113323960A, Aug.2021.

[159] Ouyang W, Li Z, Wang S T. Magnetic gradient and array arrangement of large load-bearing magneto-hydraulic double-floating radial bearings. CN113048150A, Jun.2021.

[160] Wang Z Q, Ni J, Gao D R. Combined effect of the use of carbon fiber and seawater and the molecular structure on the tribological behavior of polymer materials. *Friction* **6**(2): 183–194 (2018)

[161] Sviridyonk A I. Self-lubrication mechanisms in polymer composites. *Tribol Int* **24**(1): 37–43 (1991)

[162] Sutton D C, Limbert G, Stewart D, Wood R J K. The friction of diamond-like carbon coatings in a water environment. *Friction* **1**(3): 210–221 (2013)

[163] Li C J, Tang W W, Tang X Z, Yang L Y, Bai L C. A molecular dynamics study on the synergistic lubrication mechanisms of graphene/water-based lubricant systems. *Tribol Int* **167**: 107356 (2022)

[164] Dong C L, Yuan C Q, Wang L, Liu W, Bai X Q, Yan X P. Tribological properties of water-lubricated rubber materials after modification by MoS_2 nanoparticles. *Sci Rep* **6**: 35023 (2016)

[165] Wang C, Zhou X C, Kuang F M, Huang J, Wang H. Effect of carbon nanomaterials with different dimensions on friction and wear properties of water-lubricated rubber bearings. *Lubr Eng* **45**(02): 35–39 (2020) (in Chinese)

[166] Gao C P, Guo G F, Zhang G, Wang Q H, Wang T M, Wang H G. Formation mechanisms and functionality of boundary films derived from water lubricated polyoxymethylene/hexagonal boron nitride nanocomposites. *Mater Des* **115**: 276–286 (2017)

[167] Yan Z M, Zhou X C, Qin H L, Niu W Y, Wang H, Liu K, Tang Y M. Study on tribological and vibration performance of a new UHMWPE/graphite/NBR water lubricated bearing material. *Wear* **332–333**: 872–878 (2015)

[168] Liu X S, Zhou X C, Yang C Z, Huang J, Kuang F M, Wang H. Study on the effect of particle size and dispersion of SiO_2 on tribological properties of nitrile rubber. *Wear* **460–461**: 203428 (2020)

[169] Liu X S, Zhou X C, Kuang F M, Zuo H X, Huang J. Mechanical and tribological properties of nitrile rubber reinforced by nano-SiO_2: Molecular dynamics simulation. *Tribol Lett* **69**(2): 1–11 (2021)

[170] Qu C H, Wang T M, Wang Q H, Chen S B. A novel ternary interpenetrating polymer networks based on NBR/PU/EP with outstanding damping and tribological properties for water-lubricated bearings. *Tribol Int* **167**: 107249 (2022)

[171] Dong C L, Yuan C Q, Bai X Q, Tian Y. A novel approach to reduce deformation behaviors of HDPE polymer during friction. *Appl Surf Sci* **503**: 144311 (2020)

[172] Li S F, Dong C L, Yuan C Q, Liu S T, Bai X Q. Effects of CeO_2 nano-particles on anti-aging performance of HDPE polymer during friction. *Wear* **477**: 203832 (2021)

[173] Zhang L Y, Yuan C Q, Dong C L, Wu Y H, Bai X Q. Friction-induced vibration and noise behaviors of a composite material modified by graphene nano-sheets. *Wear* **476**: 203719 (2021)

[174] Cui Z T, Guo Z W, Xie X, Yuan C Q. The synergistic effect mechanism of pa66 self-lubrication property and surface texture on tribological performance of hdpe water-lubricated bearing. *Tribology* **39**(04): 407-417 (2019)

[175] Xie X, Guo Z W, Yuan C Q. Investigating the water lubrication characteristics of sisal fiber reinforced ultrahigh-molecular-weight polyethylene material. *Polym Compos* **41**(12): 5269–5280 (2020)

[176] Liang X, Guo Z W, Tian J, Yuan C Q. Development of modified polyacrylonitrile fibers for improving tribological performance characteristics of thermoplastic polyurethane material in water-lubricated sliding bearings. *Polym Adv Technol* **31**(12): 3258–3271 (2020)

[177] Wang C B, Bai X Q, Guo Z W, Dong C L, Yuan C Q. Friction and wear behaviours of polyacrylamide hydrogel microsphere/UHMWPE composite under water lubrication. *Wear* **477**: 203841 (2021)

[178] Yang Z R, Guo Z W, Yuan C Q. Tribological properties of water-lubricated stern bearing composites modified with biomimetic microcapsules. *Tribology* **38**(1): 28–36 (2018) (in Chinese)

[179] Yang Z X, Guo Z W, Yuan C Q. Tribological properties of UHMWPE composites modified with graphite-containing microcapsules for ship water-lubricated stern bearings. *Acta Armamentarii* **41**(11): 2281–2291 (2020) (in Chinese)

[180] Yang Z X, Guo Z W, Yang Z R, Wang C B, Yuan C Q. Study on tribological properties of a novel composite by filling microcapsules into UHMWPE matrix for water lubrication. *Tribol Int* **153**: 106629 (2021)

[181] Sheng C X, Wu Z M, Jiang S, Guo Z W. Tribological properties of new water-lubricated bearing materials under simulated marine environment. *Lubr Eng* **42**(4): 1–5 (2017) (in Chinese)

[182] Guo Z W, Yuan C Q, Liu A X, Jiang S, Tao W. Study on self-lubricating performance of water-lubricated stern tube bearing materials based on bionics. *Lubr Eng* **41**(11): 124–128, 140 (2016) (in Chinese)

[183] Guo Z W, Yuan C Q, Liu A X, Jiang S. Study on tribological properties of novel biomimetic material for water-lubricated stern tube bearing. *Wear* **376–377**: 911–919 (2017)

[184] Abdel-Aal H A, Mansori M E, Zahouani H. A comparative study of frictional response of shed snakeskin and human skin. *Wear* **376–377**: 281–294 (2017)

[185] Abdel-Aal H A. On surface structure and friction regulation in reptilian limbless locomotion. *J Mech Behav Biomed Mater* **22**: 115–135 (2013)

[186] Burris D L, Moore A C. Cartilage and joint lubrication: New insights into the role of hydrodynamics. *Biotribology* **12**: 8–14 (2017)

[187] Gao F G, Baraka-Kamali E, Shirtcliffe N, Terrell-Nield C. A preliminary study of the surface properties of earthworms and their relations to non-stain behaviour. *J Bionic Eng* **7**(1): 13–18 (2010)

[188] Zhao H, Sun Q, Deng X, Cui J. Earthworm-inspired rough polymer coatings with self-replenishing lubrication for adaptive friction-reduction and antifouling surfaces. *Adv Mater* **30**: e1802141 (2018)

[189] Zhang D G, Chen Y X, Ma Y H, Guo L, Sun J Y, Tong J. Earthworm epidermal mucus: Rheological behavior reveals drag-reducing characteristics in soil. *Soil Tillage Res* **158**: 57–66 (2016)

[190] Li X F, Guo Z W, Huang Q R, Yuan C Q. Application of bionic tribology in water-lubricated bearing: A review. *J Bionic Eng* **19**(4): 902–934 (2022)

[191] Kaur M, Gautam S, Goyal N. Ion-implantation and photovoltaics efficiency: A review. *Mater Lett* **309**: 131356 (2022)

[192] Luo S Y, Yuan Z T. Application and research progress of ion implantation technology in surface modification for materials. *Hot Work Technol* **47**(4): 43–46, 50 (2018) (in Chinese)

[193] Nenadović M, Potočnik J, Ristić M, Štrbac S, Rakočević Z. Surface modification of polyethylene by Ag+ and Au+ ion implantation observed by phase imaging atomic force microscopy. *Surf Coat Technol* **206**(19–20): 4242–4248 (2012)

[194] Feng X G, Zhang K F, Zhou H, Zheng Y G, Wan Z H. Characterization of Ti_6Al_4V alloy with N+C, Ti+N and Ti+C ion implantation. *Rare Met Mater Eng* **48**(5): 1447–1453 (2019) (in Chinese)

[195] Li C, Cheng Y, Zhong L, Yu X, Wang Y. Application of ion implantation technology in surface modification of medical titanium and its alloys. *Surf Technol* **49**(7) 49(7): 28–34 (2020) (in Chinese)

[196] Arif S, Saleem S, Murtaza G, Ayub R, Mahmood A, Anwar M S. Investigations of N+-ion implanted polymethylmethacrylate for flexible electronics. *Opt Mater* **129**: 112521 (2022)

[197] Peng E G, Liu Z L, Zhou X C, Zhao M Y, Lan F. Application of vibration and noise analysis in water-lubricated rubber bearings fault diagnosis. *Adv Mater Res* **328–330**: 1995–1999 (2011)

[198] Drummond C, Israelachvili J, Richetti P. Friction between two weakly adhering boundary lubricated surfaces in water. *Phys Rev E Stat Nonlin Soft Matter Phys* **67**(6 pt 2): 066110 (2003)

[199] Schallamach A. How does rubber slide? *Wear* **17**(4): 301–312 (1971)

[200] Schallamach A. A theory of dynamic rubber friction. *Wear* **6**(5): 375–382 (1963)

[201] Dong C L, Yuan C Q, Bai X Q, Yan X P, Peng Z X. Study on wear behaviour and wear model of nitrile butadiene rubber under water lubricated conditions. *RSC Adv* **4**(36): 19034–19042 (2014)

[202] Dong C L. Study on friction and wear mechanism and wear life prediction of water lubricated rubber stern bearing material. Ph.D. Thesis. Wuhan (China): Wuhan University of Technology, 2015.

[203] Huang J, Zhou X C, Wang J, Tang X W, Kuang F M. Influence of temperature on friction of polymeric materials in water. *Wear* **426–427**: 868–876 (2019)

[204] Yuan C Q, Guo Z W, Tao W, Dong C L, Bai X Q. Effects of different grain sized sands on wear behaviours of NBR/casting copper alloys. *Wear* **384–385**: 185–191 (2017)

[205] Dong C L, Yuan C Q, Bai X Q, Yang Y, Yan X P. Study on wear behaviours for NBR/stainless steel under sand water-lubricated conditions. *Wear* **332–333**: 1012–1020 (2015)

[206] Yang C Z, Zhou X C, Huang J, Kuang F M, Liu X S. Effects of sediment size and type on the tribological properties of NBR in water. *Wear* **477**: 203800 (2021)

[207] Liang X X, Yang Z Y. Experimental study on the influence of friction pair material hardness on the tribological behaviors of water lubricated thrust bearings. *Ind Lubr Tribol* **73**(6): 929–936 (2021)

[208] Ning C X, Zhang X Q, Yan X P, Wu O Y, Xu D L. Accelerated wear test and failure mechanism analysis of PEEK water-lubricated thrust Bearing. In *the 6th International Conference on Transportation Information and Safety (ICTIS 2021)*, Wuhan, China, IEEE, 2021: 278–284

[209] Inoue K, Deguchi K, Okude K, Fujimoto R. Development of the water-lubricated thrust bearing of the hydraulic turbine generator. *IOP Conf Ser Earth Environ Sci* **15**(7): 072022 (2012)

[210] Rey T, Chagnon G, le Cam J B, Favier D. Influence of the temperature on the mechanical behaviour of filled and unfilled silicone rubbers. *Polym Test* **32**(3): 492–501 (2013)

[211] Hirani H, Verma M. Tribological study of elastomeric bearings for marine propeller shaft system. *Tribol Int* **42**(2): 378–390 (2009)

[212] Dong C L, Yuan C Q, Bai X Q, Yan X P, Peng Z. Tribological properties of aged nitrile butadiene rubber under dry sliding conditions. *Wear* **322–323**: 226–237 (2015)

[213] Dong C L, Yuan C Q, Xu A J, Bai X Q, Tian Y. Rippled polymer surface generated by stick–slip friction. *Langmuir* **35**(7): 2878–2884 (2019)

[214] Liang X, Guo Z W, Jun T, Yuan C Q. Effect of modified glass fiber on tribological performance of water-lubricated bearing. *Polym Test* **81**: 106153 (2020)

[215] Chen B B, Wang J Z, Yan F Y. Comparative investigation on the tribological behaviors of CF/PEEK composites under sea water lubrication. *Tribol Int* **52**: 170–177 (2012)

[216] Xie G Y, Zhong Y J, Sui G X, Yang R. Mechanical properties and sliding wear behavior of potassium titanate whiskers-reinforced poly(ether ether ketone) composites under water-lubricated condition. *J Appl Polym Sci* **117**(1): 186–193 (2010)

[217] Chukov D I, Stepashkin A A, Maksimkin A V, Tcherdyntsev V V, Kaloshkin S D, Kuskov K V, Bugakov V I. Investigation of structure, mechanical and tribological properties of short carbon fiber reinforced UHMWPE-matrix composites. *Compos B Eng* **76**: 79–88 (2015)

[218] Kuang F M, Zhou X C, Huang J, Zhou X R, Wang J. Tribological properties of nitrile rubber/UHMWPE/nano-MoS_2 water-lubricated bearing material under low speed and heavy duty. *J Tribol* **140**(6): 061301 (2018)

[219] Yamamoto Y, Takashima T. Friction and wear of water lubricated PEEK and PPS sliding contacts. *Wear* **253**(7–8): 820–826 (2002)

[220] Meicke S, Paasch R. Seawater lubricated polymer journal bearings for use in wave energy converters. *Renew Energy* **39**(1): 463–470 (2012)

[221] Mu L W, Feng X, Shi Y J, Wang H Y, Lu X H. Friction and wear behaviors of solid lubricants/polyimide composites in liquid mediums. *Mater Sci Forum* **654–656**: 2763–2766 (2010)

[222] Guo Q B, Rong M Z, Jia G L, Lau K T, Zhang M Q. Sliding wear performance of nano-SiO_2/short carbon fiber/epoxy hybrid composites. *Wear* **266**(7–8): 658–665 (2009)

[223] Chang L, Friedrich K. Enhancement effect of nanoparticles on the sliding wear of short fiber-reinforced polymer composites: A critical discussion of wear mechanisms. *Tribol Int* **43**(12): 2355–2364 (2010)

[224] Xie G Y, Sui G X, Yang R. Effects of potassium titanate whiskers and carbon fibers on the wear behavior of polyetheretherketone composite under water lubricated condition. *Compos Sci Technol* **71**(6): 828–835 (2011)

[225] Chen B B, Wang J Z, Liu N, Yan F Y. Synergism of several carbon series additions on the microstructures and tribological behaviors of polyimide-based composites under sea water lubrication. *Mater Des* **63**: 325–332 (2014)

[226] Golchin A, Friedrich K, Noll A, Prakash B. Tribological behavior of carbon-filled PPS composites in water lubricated contacts. *Wear* **328–329**: 456–463 (2015)

[227] Xuan J L, Hong I T, Fitch E C. Hardness effect on three-body abrasive wear under fluid film lubrication. *J Tribol* **111**(1): 35–40 (1989)

[228] Wang Y X, Wang L P, Xue Q J. Improvement in the tribological performances of Si_3N_4, SiC and WC by graphite-like carbon films under dry and water-lubricated sliding conditions. *Surf Coat Technol* **205**(8–9): 2770–2777 (2011)

[229] Wang Q Z, Zhou F, Zhu L, Zhang M D. Tribological dependence of CrSiBCN composite coatings on different counterparts in water lubrication. *J Mater Eng Perform* **29**(1): 456–463 (2020)

[230] Wang Q Z, Zhou F, Zhou Z F, Yang Y, Yan C, Wang C D, Zhang W J, Li L K Y, Bello I, Lee S T. Influence of carbon content on the microstructure and tribological properties of TiN(C) coatings in water lubrication. *Surf Coat Technol* **206**(18): 3777–3787 (2012)

[231] Wang Q Z, Zhou F, Zhou Z F, Yang Y, Yan C, Wang C D, Zhang W J, Li L K Y, Bello I, Lee S T. Influence of Ti content on the structure and tribological properties of Ti-DLC coatings in water lubrication. *Diam Relat Mater* **25**: 163–175 (2012)

[232] Wu Z W, Zhou F, Wang Q Z, Zhou Z F, Yan J W, Li L K Y. Influence of trimethylsilane flow on the microstructure, mechanical and tribological properties of CrSiCN coatings in water lubrication. *Appl Surf Sci* **355**: 516–530 (2015)

[233] Wei S B, Pei X H, Shi B R, Xie Y, Shao T M, Shang H F. Friction performance of WC-Co coating with lithium grease and water lubrication. *Int J Surf Sci Eng* **10**(3): 272 (2016)

[234] Zhang C Q, Fujii M. Tribological behavior of thermally sprayed WC coatings under water lubrication. *Mater Sci Appl* **7**(9): 527–541 (2016)

[235] Cui R X, Li M Y, Wang H F. Wear and erosion-corrosion behaviors of ion-nitrided 2Cr13 stainless steel. *Heat Treat* **24**(3): 55–57 (2009) (in Chinese)

[236] Tang Q G, Chen J S, Andrea V. Tribological behaviors of carbon fiber-reinforced PEEK sliding on ion-nitrided 2Cr13 steel lubricated with tap water. *Tribol Trans* **58**(4): 691–697 (2015)

[237] Lv M, Wang L T, Liu J, Kong F D, Ling A X, Wang T M, Wang Q H. Surface energy, hardness, and tribological properties of carbon-fiber/polytetrafluoroethylene composites modified by proton irradiation. *Tribol Int* **132**: 237–243 (2019)

[238] Jia Z M, Guo Z W, Yuan C Q. Effect of material hardness on water lubrication performance of thermoplastic polyurethane under sediment environment. *J Mater Eng Perform* **30**(10): 7532–7541 (2021)

[239] Golchin A, Nguyen T D, de Baets P, Glavatskih S, Prakash B. Effect of shaft roughness and pressure on friction of polymer bearings in water. *Proc Inst Mech Eng Part J J Eng Tribol* **228**(4): 371–381 (2014)

[240] Quaglini V, Dubini P, Ferroni D, Poggi C. Influence of counterface roughness on friction properties of engineering plastics for bearing applications. *Mater Des* **30**(5): 1650–1658 (2009)

[241] Ali M, Ravens T, Petersen T, Bromaghin A, Jenson S. Impact of sediments on wear performance of critical sliding components of hydrokinetic devices. *Renew Energy* **80**: 498–507 (2015)

[242] Liao W J, Nie S L, Li L, Zhang Z H, Yuan S H. Tribological behavior of carbon fiber-reinforced PEEK sliding against engineering ceramic SiC lubricated with seawater. *Chin Hydraul & Pneum* (8): 16–19 (2015) (in Chinese)

[243] Tang Q G, Chen J T, Liu L P. Tribological behaviours of carbon fibre reinforced PEEK sliding on silicon nitride lubricated with water. *Wear* **269**(7–8): 541–546 (2010)

[244] Wang A Y, Yan S, Lin B, Zhang X F, Zhou X X. Aqueous lubrication and surface microstructures of engineering polymer materials (PEEK and PI) when sliding against Si_3N_4. *Friction* **5**(4): 414–428 (2017)

[245] Wu K, Zhou G, Mi X, Zhong P, Wang W, Liao D. Tribological and vibration properties of three different polymer materials for water-lubricated bearings. *Materials* (*Basel*) **13**(14): E3154 (2020)

[246] Liu N, Wang J Z, Chen B B, Yan F Y. Tribochemical aspects of silicon nitride ceramic sliding against stainless steel under the lubrication of seawater. *Tribol Int* **61**: 205–213 (2013)

[247] Ma J Q, Li F, Fu L C, Zhu S Y, Qiao Z H, Yang J, Liu W M. Effect of counterface on the tribological behavior of Ti_3AlC_2 at ambient. *Tribol Lett* **53**(1): 311–317 (2014)

[248] Wang S, Cheng J, Zhu S Y, Qiao Z H, Yang J, Liu W M. Frictional properties of Ti_3AlC_2 ceramic against different counterparts in deionized water and artificial seawater. *Ceram Int* **42**(3): 4578–4585 (2016)

[249] Bhushan B. Stick-slip induced noise generation in water-lubricated compliant rubber bearings. *J Lubr Technol* **102**(2): 201–210 (1980)

[250] Wu C, Chen F, Long X H. The self-excited vibration induced by friction of the shaft-hull coupled system with the water-lubricated rubber bearing and its stick-slip phenomenon. *Ocean Eng* **198**: 107002 (2020)

[251] Sinclair D. Frictional vibrations. *J Appl Mech* **22**(2): 207–214 (1955)

[252] Spurr R T. Brake squeal. In *Vibration and Noise in Motor Vehicles: A Symposium*, London, UK, 1971.

[253] Spurr R T. A theory of brake squeal. *Proc Inst Mech Eng Automob Div* **15**(1): 33–52 (1961)

[254] Liles G D. Analysis of disc brake squeal using finite element methods. *SAE Trans* **98**: 1138–1146 (1989)

[255] Hoffmann N, Fischer M, Allgaier R, Gaul L. A minimal model for studying properties of the mode-coupling type instability in friction induced oscillations. *Mech Res Commun* **29**(4): 197–205 (2002)

[256] Chen G X, Liu Q Y, Jin X S, Zhou Z R. Stability of a squealing noise model with time delay. *J Vib Shock* **27**(4): 58–62, 169 (2008) (in Chinese)

[257] Qian W J, Huang Z Q, Ouyang H, Chen G X, Yang H J. Numerical investigation of the effects of rail vibration absorbers on wear behaviour of rail surface. *Proc Inst Mech Eng Part J J Eng Tribol* **233**(3): 424–438 (2019)

[258 Rhee S K, Tsang P H S, Wang Y S. Friction-induced noise and vibration of disc brakes. *Wear* **133**(1): 39–45 (1989)

[259] Chen F, Quaglia R L, Tan C A. On automotive disc brake squeal part i: mechanisms and causes. In *SAE 2003 World*

Congress & Exhibition, SAE International, Detroit，United States, 2003.

[260] Kinkaid N M, O'Reilly O M, Papadopoulos P. On the transient dynamics of a multi-degree-of-freedom friction oscillator: A new mechanism for disc brake noise. *J Sound Vib* **287**(4–5): 901–917 (2005)

[261] Ibrahim R A. Friction-induced vibration, chatter, squeal, and chaos—part I: Mechanics of contact and friction. *Appl Mech Rev* **47**(7): 209–226 (1994)

[262] Ibrahim R A. Friction-induced vibration, chatter, squeal, and chaos—part II: Dynamics and modeling. *Appl Mech Rev* **47**(7): 227–253 (1994)

[263] Simpson T A, Ibrahim R A. Nonlinear friction-induced vibration in water-lubricated bearings. *J Vib Control* **2**(1): 87–113 (1996)

[264] Zhang Z G, Chen F, Zhang Z Y, Hua H X. Analysis of friction-induced vibration in a propeller–shaft system with consideration of bearing–shaft friction. *Proc Inst Mech Eng C J Mech Eng Sci* **228**(8): 1311–1328 (2014)

[265] Zhang Z G, Zhang Z Y, Huang X C, Hua H X. Stability and transient dynamics of a propeller-shaft system as induced by nonlinear friction acting on bearing-shaft contact interface. *J Sound Vib* **333**(12): 2608–2630 (2014)

[266] Zhang Z G, Duan N Y, Lin C G, Hua H X. Coupled dynamic analysis of a heavily-loaded propulsion shafting system with continuous bearing-shaft friction. *Int J Mech Sci* **172**: 105431 (2020)

[267] Kim S, Shin D, Palazzolo A B. A review of journal bearing induced nonlinear rotordynamic vibrations. *J Tribol* **143**(11): 1–39 (2021)

[268] Peng W C, Tan Y H. Friction-induced vibration characteristics of water-lubricated rubber bearing. *Chin J Ship Res* **13**(5): 103–107 (2018) (in Chinese)

[269] Dong C L, Shi L C, Li L Z, Bai X Q, Yuan C Q, Tian Y. Stick-slip behaviours of water lubrication polymer materials under low speed conditions. *Tribol Int* **106**: 55–61 (2017)

[270] Krauter A I. Generation of squeal/chatter in water-lubricated elastomeric bearings. *J Lubr Technol* **103**(3): 406–412 (1981)

[271] Krauter A I. Squeal of water-lubricated elastomeric bearings-an exploratory laboratory examination. In: Shaker Research Corporation Report 77-TR-25, ONR Contract No. NOOO14-74-C-O278, 1977.

[272] Smith R L. Laboratory examination of vibration induced by friction of water-lubricated compliant-layer bearings. In Shaker Research Corporation Report 76 - Tl 2 - 18, ONR Contract No. NOOOl4-74-C-0278, 1976.

[273] Jin Y, Deng T Y, Liu Z L, Zhou J H. Research on the influence of the normal vibration on the friction-induced vibration of the water-lubricated stern bearing. *J Vibroeng* **22**(4): 762–772 (2020)

[274] Peng E G, Zheng L L, Tian Y Z, Lan F. Experimental study on friction-induced vibration of water-lubricated rubber stern bearing at low speed. *Appl Mech Mater* **44–47**: 409–413 (2010)

[275] Yang J, Liu Z L, Cheng Q C, Liu X K, Deng T Y. The effect of wear on the frictional vibration suppression of water-lubricated rubber slat with/without surface texture. *Wear* **426–427**: 1304–1317 (2019)

[276] Peng E G. Study on nonlinear friction-induced vibration in water-lubricated rubber stern tube bearings. *Open Mech Eng J* **6**(1): 140–147 (2012)

[277] Han H S, Lee K H. Experimental verification of the mechanism on stick-slip nonlinear friction induced vibration and its evaluation method in water-lubricated stern tube bearing. *Ocean Eng* **182**: 147–161 (2019)

[278] Kuang F M, Zhou X C, Huang J, Wang H, Zheng P F. Machine-vision-based assessment of frictional vibration in water-lubricated rubber stern bearings. *Wear* **426–427**: 760–769 (2019)

[279] Kuang F M, Zhou X C, Liu Z L, Huang J, Liu X S, Qian K W, Gryllias K. Computer-vision-based research on friction vibration and coupling of frictional and torsional vibrations in water-lubricated bearing-shaft system. *Tribol Int* **150**: 106336 (2020)

[280] Qin H L, Yang C, Zhu H F, Li X F, Li Z X, Xu X. Experimental analysis on friction-induced vibration of water-lubricated bearings in a submarine propulsion system. *Ocean Eng* **203**: 107239 (2020)

[281] Zhou Y, Liao J, Li J B, Liu F. Effect analysis of water-lubricated bearing structure parameters on frictional noise. *J Chongqing Univ* **38**(3): 15–20 (2015) (in Chinese)

[282] Lin C G, Zou M S, Zhang H C, Qi L B, Liu S X. Influence of different parameters on nonlinear friction-induced vibration characteristics of water lubricated stern bearings. *Int J Nav Archit Ocean Eng* **13**: 746–757 (2021)

[283] Jiang H, Jiang W K. Study of lateral–axial coupling vibration of propeller-shaft system excited by nonlinear friction. *Arch Appl Mech* **86**(8): 1537–1550 (2016)

[284] Yao S W, Yang J, Zhang X B, Wang J, Rao Z S. Vibration and noise mechanism analysis and tests for water-lubrication rubber bearings. *J Vib Shock* **30**(2): 214–216 (2011) (in Chinese)

[285] Zhou X C, Kuang F M, Huang J, Liu X S, Gryllias K. Water-lubricated stern bearing rubber layer construction and material parameters: Effects on frictional vibration based on computer vision. *Tribol Trans* **64**(1): 65–81 (2021)

[286] JinY, Kuang J X, Tian X Y, Lao K S, Ouyang W, Liu Z L. Study on vibration-reduction performance of water-lubricated stern bearing with fluid-saturated perforated slab. *Chinese Journal of Ship Research* **14**(05): 58-63 (2019) (in Chinese)

[287] Ouyang W, Yan Q L, Kuang J X, Jin Y, Peng W C. Simulation and experimental investigations on water-lubricated squeeze film damping stern bearing. *J Braz Soc Mech Sci Eng* **43**(1): 1–13 (2021)

[288] Adiletta G, Della Pietra L. The squeeze film damper over four decades of investigations. Part ii: rotordynamic analyses with rigid and flexible rotors. *Shock Vibrat Digest* **34**(2): 97–126 (2002)

[289] Ouyang W, Yan Q, Liu Q, Li J. An extruded magnetic oil film water lubrication intelligent vibration damping bearing and vibration damping method. CN113833750A, Dec, 2021.

[290] Singh R K, Tiwari M, Saksena A A, Srivastava A. Analysis of a compact squeeze film damper with magneto rheological fluid. *Def Sc Jl* **70**(2): 122–130 (2020)

[291] Sheng P, Zhang X X, Liu Z, Chan C T. Locally resonant sonic materials. *Phys B Condens Matter* **338**(1–4): 201–205 (2003)

[292] Muhammad, Lim C W, Vyas N S. A novel application of multi-resonant dissipative elastic metahousing for bearings. *Acta Mech Solida Sin* **34**(4): 449–465 (2021)

[293] Qin H X, Yang D Q, Zhang X W. Vibration reduction of auxetic acoustic metamaterial mount. *J Vib Eng* **30**(6): 1012–1021 (2017) (in Chinese)

Zhuo ZHANG. He received his master degree in School of Marine Engineering in 2021 from Jimei University, Xiamen, China. Then, he has been a Ph.D. student in the School of Transportation and Logistics Engineering at Wuhan University of Technology, Wuhan, China. His research interests include optimization and performance improvement of the marine propulsion system.

Wu OUYANG. He received his Ph.D. degree in mechanical engineering from Xi'an Jiaotong University, Xi’an, China, in 2014. He is a professor of the National Engineering Research Center for Water Transport Safety, Wuhan University of Technology. His research areas cover the green and efficient propulsion technology, friction, and lubrication technology of propulsion system.

Xinping YAN. He received his Ph.D. degree in mechanical engineering from Xi'an Jiaotong University, Xi’an, China, in 1997. He is an academician of the Chinese Academy of Engineering. His current position is a professor and the director of the National Engineering Research Center for Water Transport Safety, Wuhan University of Technology. He is committed to the research on safety, intelligence, and green technology of transportation system.